

Molecular Design Based on Integer Programming and Quadratic Descriptors in a Two-layered Model

Jianshen Zhu¹, Naveed Ahmed Azam¹, Shengjuan Cao¹, Ryota Ido¹, Kazuya Haraguchi¹, Liang Zhao², Hiroshi Nagamochi¹ and Tatsuya Akutsu³

¹ Department of Applied Mathematics and Physics, Kyoto University, Kyoto 606-8501, Japan

² Graduate School of Advanced Integrated Studies in Human Survavibility (Shishu-Kan), Kyoto University, Kyoto 606-8306, Japan

³ Bioinformatics Center, Institute for Chemical Research, Kyoto University, Uji 611-0011, Japan

Abstract

A novel framework has recently been proposed for designing the molecular structure of chemical compounds with a desired chemical property, where design of novel drugs is an important topic in bioinformatics and chemo-informatics. The framework infers a desired chemical graph by solving a mixed integer linear program (MILP) that simulates the computation process of a feature function defined by a two-layered model on chemical graphs and a prediction function constructed by a machine learning method. A set of graph theoretical descriptors in the feature function plays a key role to derive a compact formulation of such an MILP. To improve the learning performance of prediction functions in the framework maintaining the compactness of the MILP, this paper utilizes the product of two of those descriptors as a new descriptor and then designs a method of reducing the number of descriptors. The results of our computational experiments suggest that the proposed method improved the learning performance for many chemical properties and can infer a chemical structure with up to 50 non-hydrogen atoms.

Keywords: Machine Learning, Integer Programming, Chemo-informatics, Materials Informatics, QSAR/QSPR, Molecular Design.

1 Introduction

Background In recent years, extensive studies have been done on design of novel molecules using various machine learning techniques [1, 2]. Computational molecular design has also a long history in the field of chemo-informatics, and has been studied under the names of *quantitative structure activity relationship* (QSAR) [3] and *inverse quantitative structure activity relationship* (inverse QSAR) [4, 5, 6]. This design problem has also become a hot topic in both bioinformatics and machine learning.

The purpose of QSAR is to predict chemical activities from given chemical structures [3]. In most of QSAR studies, a chemical structure is represented as a vector of real numbers called *features* or *descriptors* and then a prediction function is applied to the vector, where a chemical structure is given as an undirected graph called a *chemical graph*. A prediction function is usually obtained from existing structure-activity relation data. To this end, various regression-based methods have

been utilized in traditional QSAR studies, whereas machine learning-based methods, including artificial neural network (ANN)-based methods, have recently been utilized [7, 8].

Conversely, the purpose of inverse QSAR is to predict chemical structures from given chemical activities [4, 5, 6], where additional constraints may often be imposed to effectively restrict the possible structures. In traditional inverse QSAR, a feature vector is firstly computed by applying some optimization or sampling method to the prediction function obtained by usual QSAR and then chemical structures are reconstructed from the feature vector. However, the reconstruction itself is quite difficult because the number of possible chemical graphs is huge [9]. Indeed, it is NP-hard to infer a chemical graph from a given feature vector except for some simple cases [10]. Due to this inherent difficulty, most existing methods employ heuristic methods for reconstruction of chemical structures and thus do not guarantee optimal or exact solutions.

On the other hand, one of the advantages of ANNs is that generative models are available, such as autoencoders and generative adversarial networks. Furthermore, graph structured data can be directly handled by using graph convolutional networks [11]. Therefore, it is reasonable to try to apply ANNs to inverse QSAR [12]. Indeed, various ANN models have been applied, which includes recurrent neural networks [13, 14], variational autoencoders [15], grammar variational autoencoders [16], generative adversarial networks [17], and invertible flow models [18, 19]. However, optimality or exactness of the solutions is not yet guaranteed by these methods.

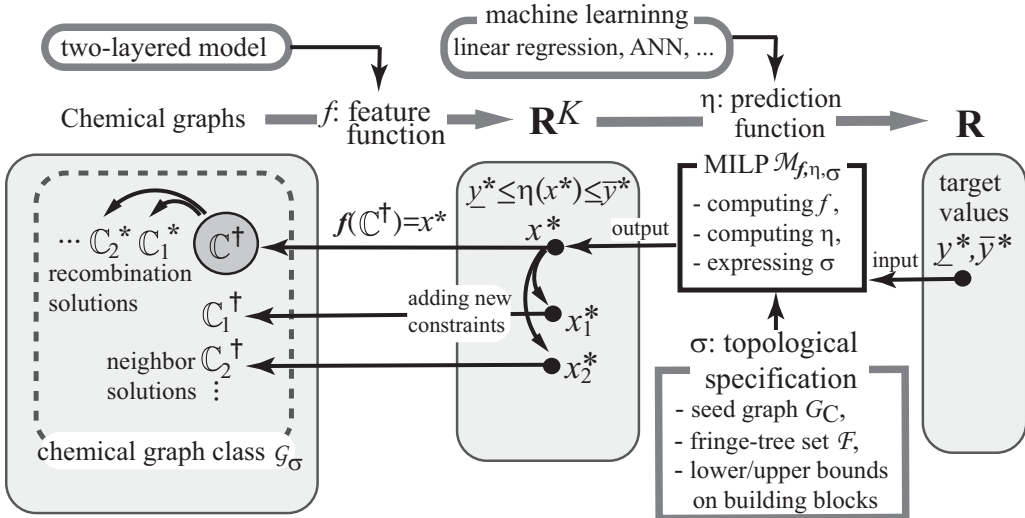


Figure 1: An illustration of inferring desired chemical graphs $\mathbb{C} \in \mathcal{G}_\sigma$ with $\underline{y}^* \leq \eta(f(\mathbb{C})) \leq \bar{y}^*$.

Framework A novel framework for inferring chemical graphs has been developed [20, 21, 22, 23] based on an idea of formulating as a mixed integer linear programming (MILP) the computation process of a prediction function constructed by a machine learning method. It consists of two main phases: the first phase constructs a prediction function η for a chemical property and the second phase infers a chemical graph with a target value of the property based on the function η . For a chemical property π , let \mathcal{C}_π be a data set of chemical graphs such that the observed value $a(\mathbb{C})$ of property π for every chemical graph $\mathbb{C} \in \mathcal{C}_\pi$ is available. In the first phase, we introduce a feature function $f : \mathcal{G} \rightarrow \mathbb{R}^K$ for a positive integer K , where the descriptors of a chemical graph

are defined based on local graph structures in a special way called a *two-layered model*. We then construct a prediction function η by a machine learning method such as linear regression, decision tree and an ANN so that the output $y = \eta(x) \in \mathbb{R}$ of the feature vector $x = f(\mathbb{C}) \in \mathbb{R}^K$ for each $\mathbb{C} \in \mathcal{C}_\pi$ serves as a predicted value to the real value $a(\mathbb{C})$. In the second phase of inferring a desired chemical graph, we specify not only a target chemical value for property π but also an abstract structure for a chemical graph to be inferred. The latter is described by a set of rules based on the two-layered model called a *topological specification* σ , and denote by \mathcal{G}_σ the set of all chemical graphs that satisfy the rules in σ . The users select topological specification σ and two reals \underline{y}^* and \overline{y}^* as an interval for a target chemical value. The task of the second phase is to infer chemical graphs $\mathbb{C}^* \in \mathcal{G}_\sigma$ such that $\underline{y}^* \leq \eta(f(\mathbb{C}^*)) \leq \overline{y}^*$ (see Figure 1 for an illustration). For this, we formulate an MILP $\mathcal{M}_{f,\eta,\sigma}$ that represents (i) the computation process of $x := f(\mathbb{C})$ from a chemical graph \mathbb{C} in the feature function f ; (ii) that of $y := \eta(x)$ from a vector $x \in \mathbb{R}^K$ in the prediction function η ; and (iii) the constraint $\mathbb{C} \in \mathcal{G}_\sigma$. Given an interval with $\underline{y}^*, \overline{y}^* \in \mathbb{R}$, we solve the MILP $\mathcal{M}_{f,\eta,\sigma}$ to find a feature vector $x^* \in \mathbb{R}^K$ and a chemical graph $\mathbb{C}^\dagger \in \mathcal{G}_\sigma$ such that $f(\mathbb{C}^\dagger) = x^*$ and $\underline{y}^* \leq \eta(x^*) \leq \overline{y}^*$ (where if the MILP instance is infeasible then this suggests that \mathcal{G}_σ does not contain such a desired chemical graph). In the second phase, we next generate some other desired chemical graphs based on the solution \mathbb{C}^\dagger . For this, the following two methods have been designed.

The first method constructs isomers of \mathbb{C}^\dagger without solving any new MILP. In this method, we first decompose the chemical graph \mathbb{C}^\dagger into a set of chemical acyclic graphs $T_1^\dagger, T_2^\dagger, \dots, T_q^\dagger$, and next construct a set \mathcal{T}_i of isomers T_i^* of each tree T_i^\dagger such that $f(T_i^*) = f(T_i^\dagger)$ by a dynamic programming algorithm due to Azam et al. [24]. Finally we choose an isomer $T_i^* \in \mathcal{T}_i$ for each $i = 1, 2, \dots, q$ and assemble them into an isomer $\mathbb{C}^* \in \mathcal{G}_\sigma$ of \mathbb{C}^\dagger such that $f(\mathbb{C}^*) = x^* = f(\mathbb{C}^\dagger)$. The first method generates such isomers $\mathbb{C}_1^*, \mathbb{C}_2^*, \dots$ which we call *recombination solutions* of \mathbb{C}^\dagger .

The second method constructs new solutions by solving the MILP $\mathcal{M}_{f,\eta,\sigma}$ with an additional set Θ of new linear constraints [23]. We first prepare arbitrary p_{dim} linear functions $\theta_j : \mathbb{R}^K \rightarrow \mathbb{R}, j = 1, 2, \dots, p_{\text{dim}}$ and consider a neighbor of \mathbb{C}^\dagger defined by a set of chemical graphs \mathbb{C}^* that satisfy linear constraints $k\delta \leq |\theta_j(f(\mathbb{C}^*)) - \theta_j(f(\mathbb{C}^\dagger))| \leq (k+1)\delta, j = 1, 2, \dots, p_{\text{dim}}$ for a small real $\delta > 0$ and an integer $k \geq 1$. By changing the integer k systematically, we can search for new solutions $\mathbb{C}_1^\dagger, \mathbb{C}_2^\dagger, \dots \in \mathcal{G}_\sigma$ of MILP $\mathcal{M}_{f,\eta,\sigma}$ with constraint Θ such that the feature vectors $x^* = f(\mathbb{C}^\dagger), x_1^* = f(\mathbb{C}_1^\dagger), x_2^* = f(\mathbb{C}_2^\dagger), \dots$ are all slightly different. We call these chemical graphs $\mathbb{C}_1^\dagger, \mathbb{C}_2^\dagger, \dots$ *neighbor solutions* of \mathbb{C}^\dagger , where a neighbor solution is not an isomer of \mathbb{C}^\dagger .

The main reason why the framework can infer a chemical compound with 50 non-hydrogen atoms is that the descriptors of a chemical graph are defined on local graph structures in the two-layered model and thereby an MILP necessary to represent a chemical graph can be formulated as a considerably compact form that is efficiently solvable by a standard solver.

Contribution In the framework, all descriptors $x(1), x(2), \dots, x(K)$ in the feature vector $x = f(\mathbb{C})$ are mainly the frequencies of local graph structures based on the two-layered model by which a chemical graph \mathbb{C} is regarded as a pair of interior and exterior structures (see Section 3 for details). To derive a compact MILP formulation to infer a chemical graph, it is important to use the current definition of descriptors. However, there are some chemical properties for which the performance of a prediction function constructed with the feature function f remains rather low. To improve

the learning performance with the same two-layered model, we add as a new descriptor the product $x(i)x(j)$ (or $x(i)(1 - x(j))$) of two descriptors (where each descriptor is assumed to be normalized within 0 and 1) and call such a new descriptor a *quadratic descriptor*. This drastically increases the number of descriptors, which would take extra running time in learning or cause overfitting to the data set. Moreover, computing quadratic descriptors cannot be directly formulated as a set of linear constraints in the original MILP. For this, we introduce a method of reducing a set of descriptors into a smaller set that delivers a prediction function with a higher performance. We also design an MILP formulation for representing a quadratic term $x(i)x(j)$. Based on the same MILP $\mathcal{M}_{f,\eta,\sigma}$ formulation proposed by Zhu et al. [21], we implemented the framework to treat the feature function with quadratic descriptors. From the results of our computational experiments on over 40 chemical properties, we observe that our new method of utilizing quadratic descriptors improved the performance of a prediction function for many chemical properties.

The paper is organized as follows. Section 2 introduces some notions on graphs and a modeling of chemical compounds. Section 3 reviews the two-layered model and a basic idea of descriptors by the model. Section 4 introduces a formulation for computing a quadratic descriptor in an MILP. Section 5 reports the results on computational experiments conducted for 42 chemical properties such as critical pressure, dissociation constants and lipophilicity for monomers and characteristic ratio and refractive index for polymers. Section 6 makes some concluding remarks. Some technical details are given in Appendices: Appendix A for all descriptors in our feature function; Appendix B for how to reduce the number of descriptors; Appendix C for a full description of a topological specification; and Appendix D for the detail of test instances used in our computational experiment.

2 Preliminary

This section introduces some notions and terminologies on graphs, modeling of chemical compounds and our choice of descriptors.

Let \mathbb{R} , \mathbb{R}_+ , \mathbb{Z} and \mathbb{Z}_+ denote the sets of reals, non-negative reals, integers and non-negative integers, respectively. For two integers a and b , let $[a, b]$ denote the set of integers i with $a \leq i \leq b$. For a vector $x \in \mathbb{R}^p$, the j -th entry of x is denoted by $x(j)$.

Graph Given a graph G , let $V(G)$ and $E(G)$ denote the sets of vertices and edges, respectively. For a subset $V' \subseteq V(G)$ (resp., $E' \subseteq E(G)$) of a graph G , let $G - V'$ (resp., $G - E'$) denote the graph obtained from G by removing the vertices in V' (resp., the edges in E'), where we remove all edges incident to a vertex in V' to obtain $G - V'$. A path with two end-vertices u and v is called a u, v -path.

We define a *rooted* graph to be a graph with a designated vertex, called a *root*. For a graph G possibly with a root, a *leaf-vertex* is defined to be a non-root vertex with degree 1. Call the edge wv incident to a leaf vertex v a *leaf-edge*, and denote by $V_{\text{leaf}}(G)$ and $E_{\text{leaf}}(G)$ the sets of leaf-vertices and leaf-edges in G , respectively. For a graph or a rooted graph G , we define graphs $G_i, i \in \mathbb{Z}_+$ obtained from G by removing the set of leaf-vertices i times so that

$$G_0 := G; \quad G_{i+1} := G_i - V_{\text{leaf}}(G_i),$$

where we call a vertex v a *tree vertex* if $v \in V_{\text{leaf}}(G_i)$ for some $i \geq 0$. Define the *height* $\text{ht}(v)$ of each tree vertex $v \in V_{\text{leaf}}(G_i)$ to be i ; and $\text{ht}(v)$ of each non-tree vertex v adjacent to a tree vertex to be $\text{ht}(u) + 1$ for the maximum $\text{ht}(u)$ of a tree vertex u adjacent to v , where we do not define height of any non-tree vertex not adjacent to any tree vertex. We call a vertex v with $\text{ht}(v) = k$ a *leaf k -branch*. The *height* $\text{ht}(T)$ of a rooted tree T is defined to be the maximum of $\text{ht}(v)$ of a vertex $v \in V(T)$.

2.1 Modeling of Chemical Compounds

We review a modeling of chemical compounds introduced by Zhu et al. [21].

To represent a chemical compound, we introduce a set of chemical elements such as H (hydrogen), C (carbon), O (oxygen), N (nitrogen) and so on. To distinguish a chemical element \mathbf{a} with multiple valences such as S (sulfur), we denote a chemical element \mathbf{a} with a valence i by $\mathbf{a}_{(i)}$, where we do not use such a suffix (i) for a chemical element \mathbf{a} with a unique valence. Let Λ be a set of chemical elements $\mathbf{a}_{(i)}$. For example, $\Lambda = \{\mathbf{H}, \mathbf{C}, \mathbf{O}, \mathbf{N}, \mathbf{P}, \mathbf{S}_{(2)}, \mathbf{S}_{(4)}, \mathbf{S}_{(6)}\}$. Let $\text{val} : \Lambda \rightarrow [1, 6]$ be a valence function. For example, $\text{val}(\mathbf{H}) = 1$, $\text{val}(\mathbf{C}) = 4$, $\text{val}(\mathbf{O}) = 2$, $\text{val}(\mathbf{P}) = 5$, $\text{val}(\mathbf{S}_{(2)}) = 2$, $\text{val}(\mathbf{S}_{(4)}) = 4$ and $\text{val}(\mathbf{S}_{(6)}) = 6$. For each chemical element $\mathbf{a} \in \Lambda$, let $\text{mass}(\mathbf{a})$ denote the mass of \mathbf{a} .

A chemical compound is represented by a *chemical graph* defined to be a tuple $\mathbb{C} = (H, \alpha, \beta)$ of a simple, connected undirected graph H and functions $\alpha : V(H) \rightarrow \Lambda$ and $\beta : E(H) \rightarrow [1, 3]$. The set of atoms and the set of bonds in the compound are represented by the vertex set $V(H)$ and the edge set $E(H)$, respectively. The chemical element assigned to a vertex $v \in V(H)$ is represented by $\alpha(v)$ and the bond-multiplicity between two adjacent vertices $u, v \in V(H)$ is represented by $\beta(e)$ of the edge $e = uv \in E(H)$. We say that two tuples $(H_i, \alpha_i, \beta_i), i = 1, 2$ are *isomorphic* if they admit an isomorphism ϕ , i.e., a bijection $\phi : V(H_1) \rightarrow V(H_2)$ such that $uv \in E(H_1), \alpha_1(u) = \mathbf{a}, \alpha_1(v) = \mathbf{b}, \beta_1(uv) = m \leftrightarrow \phi(u)\phi(v) \in E(H_2), \alpha_2(\phi(u)) = \mathbf{a}, \alpha_2(\phi(v)) = \mathbf{b}, \beta_2(\phi(u)\phi(v)) = m$. When H_i is rooted at a vertex $r_i, i = 1, 2$, these chemical graphs $(H_i, \alpha_i, \beta_i), i = 1, 2$ are *rooted-isomorphic* (r -isomorphic) if they admit an isomorphism ϕ such that $\phi(r_1) = r_2$.

For a notational convenience, we use a function $\beta_{\mathbb{C}} : V(H) \rightarrow [0, 12]$ for a chemical graph $\mathbb{C} = (H, \alpha, \beta)$ such that $\beta_{\mathbb{C}}(u)$ means the sum of bond-multiplicities of edges incident to a vertex u ; i.e.,

$$\beta_{\mathbb{C}}(u) \triangleq \sum_{uv \in E(H)} \beta(uv) \text{ for each vertex } u \in V(H).$$

For each vertex $u \in V(H)$, define the *electron-degree* $\text{eledeg}_{\mathbb{C}}(u)$ to be

$$\text{eledeg}_{\mathbb{C}}(u) \triangleq \beta_{\mathbb{C}}(u) - \text{val}(\alpha(u)).$$

For each vertex $u \in V(H)$, let $\text{deg}_{\mathbb{C}}(v)$ denote the number of vertices adjacent to u in \mathbb{C} .

For a chemical graph $\mathbb{C} = (H, \alpha, \beta)$, let $V_{\mathbf{a}}(\mathbb{C}), \mathbf{a} \in \Lambda$ denote the set of vertices $v \in V(H)$ such that $\alpha(v) = \mathbf{a}$ in \mathbb{C} and define the *hydrogen-suppressed chemical graph* $\langle \mathbb{C} \rangle$ to be the graph obtained from H by removing all the vertices $v \in V_{\mathbf{H}}(\mathbb{C})$.

2.2 Prediction Functions

Let \mathcal{C} be a data set of chemical graphs \mathbb{C} with an observed value $a(\mathbb{C}) \in \mathbb{R}$. Let D be a set of descriptors and f be a feature function that maps a chemical graph \mathbb{C} to a vector $f(\mathbb{C}) \in \mathbb{R}^D$, where $x(d)$ denotes the value of descriptor $d \in D$. For a notational simplicity, we denote $a_i = a(\mathbb{C}_i)$ and $x_i = f(\mathbb{C}_i)$ for an indexed graph $\mathbb{C}_i \in \mathcal{C}$.

2.2.1 Evaluation

For a prediction function $\eta : \mathbb{R}^D \rightarrow \mathbb{R}$, define an error function

$$\text{Err}(\eta; \mathcal{C}) \triangleq \sum_{\mathbb{C}_i \in \mathcal{C}} (a_i - \eta(f(\mathbb{C}_i)))^2 = \sum_{\mathbb{C}_i \in \mathcal{C}} (a_i - \eta(x_i))^2,$$

and define the *coefficient of determination* $R^2(\eta, \mathcal{C})$ to be

$$R^2(\eta, \mathcal{C}) \triangleq 1 - \frac{\text{Err}(\eta; \mathcal{C})}{\sum_{\mathbb{C}_i \in \mathcal{C}} (a_i - \tilde{a})^2} \text{ for } \tilde{a} = \frac{1}{|\mathcal{C}|} \sum_{\mathbb{C} \in \mathcal{C}} a(\mathbb{C}).$$

We evaluate a method of constructing a prediction function over a set D of descriptors by 5-fold cross-validation as follows. A single run r of 5-fold cross-validation executes the following: Partition a data set \mathcal{C} randomly into five subsets $\mathcal{C}^{(k)}$, $k \in [1, 5]$ so that the difference between $|\mathcal{C}^{(i)}|$ and $|\mathcal{C}^{(j)}|$ is at most 1. For each $k \in [1, 5]$, let $\mathcal{C}_{\text{train}} := \mathcal{C} \setminus \mathcal{C}^{(k)}$, $\mathcal{C}_{\text{test}} := \mathcal{C}^{(k)}$ and execute the method to construct a prediction function $\eta^{(k)} : \mathbb{R}^D \rightarrow \mathbb{R}$ over a training set $\mathcal{C}_{\text{train}}$ and compute $g_r^{(k)} := R^2(\eta^{(k)}, \mathcal{C}_{\text{test}})$. Let $R_{\text{CV}}^2(\mathcal{C}, D, p)$ denote the median of $\{g_{r_i}^{(k)} \mid k \in [1, 5], i \in [1, p]\}$ of p runs r_1, r_2, \dots, r_p of 5-fold cross-validation.

2.2.2 Linear regressions

For a set D of descriptors, a hyperplane is defined to be a pair (w, b) of a vector $w \in \mathbb{R}^D$ and a real $b \in \mathbb{R}$. Given a hyperplane (w, b) , a prediction function $\eta_{w,b} : \mathbb{R}^D \rightarrow \mathbb{R}$ is defined by setting

$$\eta_{w,b}(x) \triangleq w \cdot x + b = \sum_{d \in D} w(d)x(d) + b.$$

Given a data set \mathcal{C} and a set D of descriptors, *multidimensional linear regression* $\text{MLR}(\mathcal{C}, D)$ returns a hyperplane (w, b) with $w \in \mathbb{R}^D$ that minimizes $\text{Err}(\eta_{w,b}; \mathcal{C})$. However, such a hyperplane (w, b) may contain unnecessarily many non-zero reals $w(d)$. To avoid this, a minimization with an additional penalty term τ to the error function has been proposed. Among them, a Lasso function [25] is defined to be

$$\frac{1}{2|\mathcal{C}|} \text{Err}(\eta_{w,b}; \mathcal{C}) + \lambda\tau, \quad \tau = \sum_{d \in D} |w(d)| + |b|,$$

where $\lambda \in \mathbb{R}$ is a given nonnegative number.

Given a data set \mathcal{C} , a set D of descriptors and a real $\lambda > 0$, let $\text{LLR}(\mathcal{C}, D, \lambda)$ be a procedure that returns a hyperplane $(w \in \mathbb{R}^D, b)$ that minimizes the above function.

We review a recent learning method, called *adjustive linear regression*, that is effectively equivalent to an ANN with no hidden layers by a linear regression such that each input node may have a non-linear activation function (see [26] for the details of the idea). Let $\mathcal{C} = \{\mathbb{C}_1, \mathbb{C}_2, \dots, \mathbb{C}_m\}$, $A = \{a_i = f(\mathbb{C}_i) \mid i \in [1, m]\}$ and $X = \{x_i = f(\mathbb{C}_i) \in \mathbb{R}^D \mid i \in [1, m]\}$. Let D^+ (resp., D^-) denote the set of descriptor $d \in D$ such that the correlation coefficient $\sigma(X[d], A)$ between $X[d] = \{x_i(d) \mid i \in [1, m]\}$ and A is nonnegative (resp., negative). We first solve the following minimization problem with a constant $\lambda \geq 0$, a real variable b and nonnegative real variables $c_q(0), q \in [0, 2]$, $w_q(d), q \in [0, 2], d \in D$.

Adjustive Linear Regression(\mathcal{C}, λ)

$$\begin{aligned} \text{Minimize: } \frac{1}{2m} \sum_{i \in [1, m]} & \left| c_0(0)a_i + c_1(0)a_i^2 + c_2(0)(1 - (a_i - 1)^2) \right. \\ & - \sum_{d \in D^+} [w_0(d)x_i(d) + w_1(d)x_i(d)^2 + w_2(d)(1 - (x_i(d) - 1)^2)] \\ & \left. + \sum_{d \in D^-} [w_0(d)x_i(d) + w_1(d)x_i(d)^2 + w_2(d)(1 - (x_i(d) - 1)^2)] - b \right| + \lambda \tau \end{aligned}$$

subject to

$$\tau = \sum_{d \in D} w_0(d) + |b|, \quad c_0(0) + c_1(0) + c_2(0) = 1. \tag{1}$$

An optimal solution to this minimization can be found by solving a linear program with $O(m + |D|)$ variables and constraints. From an optimal solution, we next compute the following hyperplane (w^*, b^*) to obtain a linear prediction function η_{w^*, b^*} . Let $c_q^*(0), q \in [0, 2]$, $w_q^*(d), q \in [0, 2], d \in D$ and b^* denote the values of variables $c_q(0), q \in [0, 2]$, $w_q(d), q \in [0, 2], d \in D$ and b in an optimal solution, respectively. Let D^\dagger denote the set of descriptors $d \in D$ with $w_0^*(d) > 0$. Then we set $w^*(d) := 0$ for $d \in D$ with $w_0^*(d) = 0$, $w^*(d) := w_0^*(d)/(w_0^*(d) + w_1^*(d) + w_2^*(d))$ for $d \in D^+ \cap D^\dagger$, $w^*(d) := -w_0^*(d)/(w_0^*(d) + w_1^*(d) + w_2^*(d))$ for $d \in D^- \cap D^\dagger$ and $w^* := (w_0^*(1), w_0^*(2), \dots, w_0^*(|D|)) \in \mathbb{R}^D$.

3 Two-layered Model

This section reviews the two-layered model introduced by Shi et al. [20].

Let $\mathbb{C} = (H, \alpha, \beta)$ be a chemical graph and $\rho \geq 1$ be an integer, which we call a *branch-parameter*.

A *two-layered model* of \mathbb{C} is a partition of the hydrogen-suppressed chemical graph $\langle \mathbb{C} \rangle$ into an ‘‘interior’’ and an ‘‘exterior’’ in the following way. We call a vertex $v \in V(\langle \mathbb{C} \rangle)$ (resp., an edge $e \in E(\langle \mathbb{C} \rangle)$) of \mathbb{C} an *exterior-vertex* (resp., *exterior-edge*) if $\text{ht}(v) < \rho$ (resp., e is incident to an exterior-vertex) and denote the sets of exterior-vertices and exterior-edges by $V^{\text{ex}}(\mathbb{C})$ and $E^{\text{ex}}(\mathbb{C})$, respectively and denote $V^{\text{int}}(\mathbb{C}) = V(\langle \mathbb{C} \rangle) \setminus V^{\text{ex}}(\mathbb{C})$ and $E^{\text{int}}(\mathbb{C}) = E(\langle \mathbb{C} \rangle) \setminus E^{\text{ex}}(\mathbb{C})$, respectively. We call a vertex in $V^{\text{int}}(\mathbb{C})$ (resp., an edge in $E^{\text{int}}(\mathbb{C})$) an *interior-vertex* (resp., *interior-edge*). The set $E^{\text{ex}}(\mathbb{C})$ of exterior-edges forms a collection of connected graphs each of which is regarded as a rooted tree T rooted at the vertex $v \in V(T)$ with the maximum $\text{ht}(v)$. Let $\mathcal{T}^{\text{ex}}(\langle \mathbb{C} \rangle)$ denote

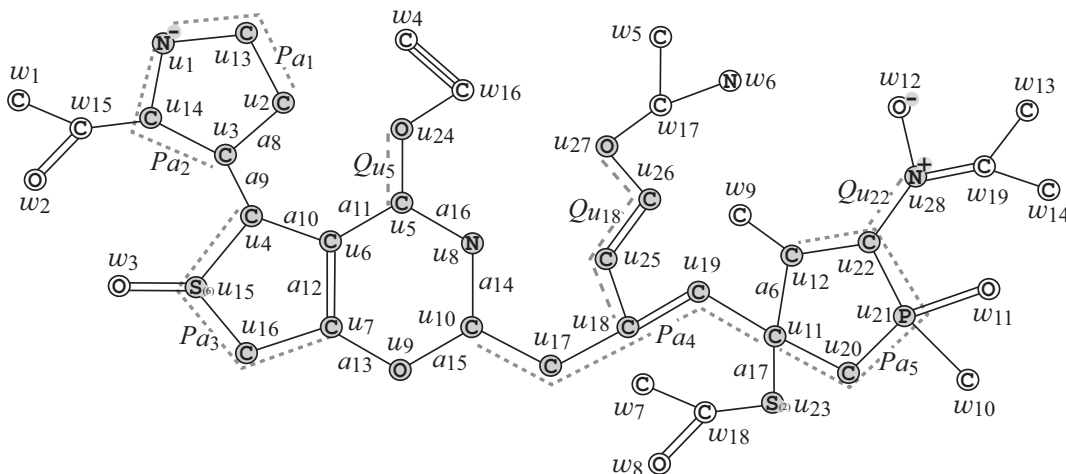


Figure 2: An illustration of a hydrogen-suppressed chemical graph $\langle \mathbb{C} \rangle$ obtained from a chemical graph \mathbb{C} by removing all the hydrogens, where for $\rho = 2$, $V^{\text{ex}}(\mathbb{C}) = \{w_i \mid i \in [1, 19]\}$ and $V^{\text{int}}(\mathbb{C}) = \{u_i \mid i \in [1, 28]\}$.

the set of these chemical rooted trees in $\langle \mathbb{C} \rangle$. The *interior* \mathbb{C}^{int} of \mathbb{C} is defined to be the subgraph $(V^{\text{int}}(\mathbb{C}), E^{\text{int}}(\mathbb{C}))$ of $\langle \mathbb{C} \rangle$.

Figure 2 illustrates an example of a hydrogen-suppressed chemical graph $\langle \mathbb{C} \rangle$. For a branch-parameter $\rho = 2$, the interior of the chemical graph $\langle \mathbb{C} \rangle$ in Figure 2 is obtained by removing the set of vertices with degree 1 $\rho = 2$ times; i.e., first remove the set $V_1 = \{w_1, w_2, \dots, w_{14}\}$ of vertices of degree 1 in $\langle \mathbb{C} \rangle$ and then remove the set $V_2 = \{w_{15}, w_{16}, \dots, w_{19}\}$ of vertices of degree 1 in $\langle \mathbb{C} \rangle - V_1$, where the removed vertices become the exterior-vertices of $\langle \mathbb{C} \rangle$.

For each interior-vertex $u \in V^{\text{int}}(\mathbb{C})$, let $T_u \in \mathcal{T}^{\text{ex}}(\langle \mathbb{C} \rangle)$ denote the chemical tree rooted at u (where possibly T_u consists of vertex u) and define the ρ -fringe-tree $\mathbb{C}[u]$ to be the chemical rooted tree obtained from T_u by putting back the hydrogens originally attached T_u in \mathbb{C} . Let $\mathcal{T}(\mathbb{C})$ denote the set of ρ -fringe-trees $\mathbb{C}[u]$, $u \in V^{\text{int}}(\mathbb{C})$. Figure 3 illustrates the set $\mathcal{T}(\mathbb{C}) = \{\mathbb{C}[u_i] \mid i \in [1, 28]\}$ of the 2-fringe-trees of the example \mathbb{C} in Figure 2.

Feature Function The feature of an interior-edge $e = uv \in E^{\text{int}}(\mathbb{C})$ such that $\alpha(u) = \mathbf{a}$, $\deg_{\langle \mathbb{C} \rangle}(u) = d$, $\alpha(v) = \mathbf{b}$, $\deg_{\langle \mathbb{C} \rangle}(v) = d'$ and $\beta(e) = m$ is represented by a tuple $(\mathbf{a}d, \mathbf{b}d', m)$, which is called the *edge-configuration* of the edge e , where we call the tuple $(\mathbf{a}, \mathbf{b}, m)$ the *adjacency-configuration* of the edge e .

In the framework with the two-layered model, the feature vector f mainly consists of the frequency of edge-configurations of the interior-edges and the frequency of chemical rooted trees among the set of chemical rooted trees $\mathbb{C}[u]$ over all interior-vertices u . See Appendix A for all these descriptors $x(1), x(2), \dots, x(K_1)$, which are called *linear descriptors*. We denote by $D_\pi^{(1)} := \{x(k) \mid k \in [1, K_1]\}$ the set of descriptors constructed over a data set for a property π . In this paper, we also use a quadratic term $x(i)x(j)$ (or $x(i)(1 - x(j))$), $1 \leq i \leq j \leq K_1$ as a new descriptor, where we assume that each $x(i)$ is normalized between 0 and 1. We call such a term $x(i)x(j)$ (or $x(i)(1 - x(j))$), $1 \leq i \leq j \leq K_1$ a *quadratic descriptor* and denote by $D_\pi^{(2)} := \{x(i)x(j) \mid 1 \leq i \leq j \leq K_1\} \cup \{x(i)(1 - x(j)) \mid 1 \leq i, j \leq K_1\}$ the set of quadratic descriptors.

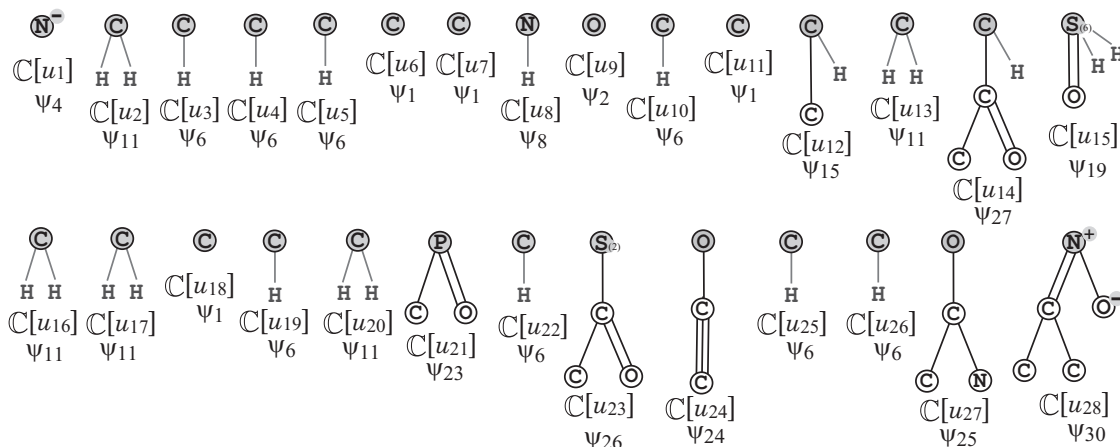


Figure 3: The set $\mathcal{T}(\mathbb{C})$ of 2-fringe-trees $\mathbb{C}[u_i]$, $i \in [1, 28]$ of the example \mathbb{C} in Figure 2, where the root of each tree is depicted with a gray circle and the hydrogens attached to non-root vertices are omitted in the figure.

To construct a prediction function, we use the union $D_\pi^{(1)} \cup D_\pi^{(2)}$. This set of descriptors is usually excessive in constructing a prediction function, and we reduce it to a smaller set of descriptors to construct a *feature function* $f: \mathbb{R}^K \rightarrow \mathbb{R}$, where K is the number of resulting descriptors. We call \mathbb{R}^K the *feature space*. See Appendix B for methods of reducing descriptors.

Topological Specification A topological specification σ is described as a set of the following rules:

- (i) a *seed graph* G_C as an abstract form of a target chemical graph \mathbb{C} ;
- (ii) a set \mathcal{F} of chemical rooted trees as candidates for a tree $\mathbb{C}[u]$ rooted at each exterior-vertex u in \mathbb{C} ; and
- (iii) lower and upper bounds on the number of components in a target chemical graph such as chemical elements, double/triple bonds and the interior-vertices in \mathbb{C} .

Figures 4(a) and (b) illustrate examples of a seed graph G_C and a set \mathcal{F} of chemical rooted trees, respectively. Given a seed graph G_C , the interior of a target chemical graph \mathbb{C} is constructed from G_C by replacing some edges $a = uv$ with paths P_a between the end-vertices u and v and by attaching new paths Q_v to some vertices v . For example, a chemical graph \mathbb{C} in Figure 2 is constructed from the seed graph G_C in Figure 4(a) as follows.

- First replace five edges $a_1 = u_1u_2$, $a_2 = u_1u_3$, $a_3 = u_4u_7$, $a_4 = u_{10}u_{11}$ and $a_5 = u_{11}u_{12}$ in G_C with new paths $P_{a_1} = (u_1, u_{13}, u_2)$, $P_{a_2} = (u_1, u_{14}, u_3)$, $P_{a_3} = (u_4, u_{15}, u_{16}, u_7)$, $P_{a_4} = (u_{10}, u_{17}, u_{18}, u_{19}, u_{11})$ and $P_{a_5} = (u_{11}, u_{20}, u_{21}, u_{22}, u_{12})$, respectively to obtain a subgraph G_1 of $\langle \mathbb{C} \rangle$.
- Next attach to this graph G_1 three new paths $Q_{u_5} = (u_5, u_{24})$, $Q_{u_{18}} = (u_{18}, u_{25}, u_{26}, u_{27})$ and $Q_{u_{22}} = (u_{22}, u_{28})$ to obtain the interior of $\langle \mathbb{C} \rangle$ in Figure 2.
- Finally attach to the interior 28 trees selected from the set \mathcal{F} and assign chemical elements and bond-multiplicities in the interior to obtain a chemical graph \mathbb{C} in Figure 2. In Figure 3, $\psi_1 \in \mathcal{F}$ is selected for $\mathbb{C}[u_i]$, $i \in \{6, 7, 11\}$. Similarly ψ_2 for $\mathbb{C}[u_9]$, ψ_4 for $\mathbb{C}[u_1]$, ψ_6 for $\mathbb{C}[u_i]$, $i \in \{3, 4, 5, 10, 19, 22, 25, 26\}$, ψ_8 for $\mathbb{C}[u_8]$, ψ_{11} for $\mathbb{C}[u_i]$, $i \in \{2, 13, 16, 17, 20\}$, ψ_{15} for $\mathbb{C}[u_{12}]$,

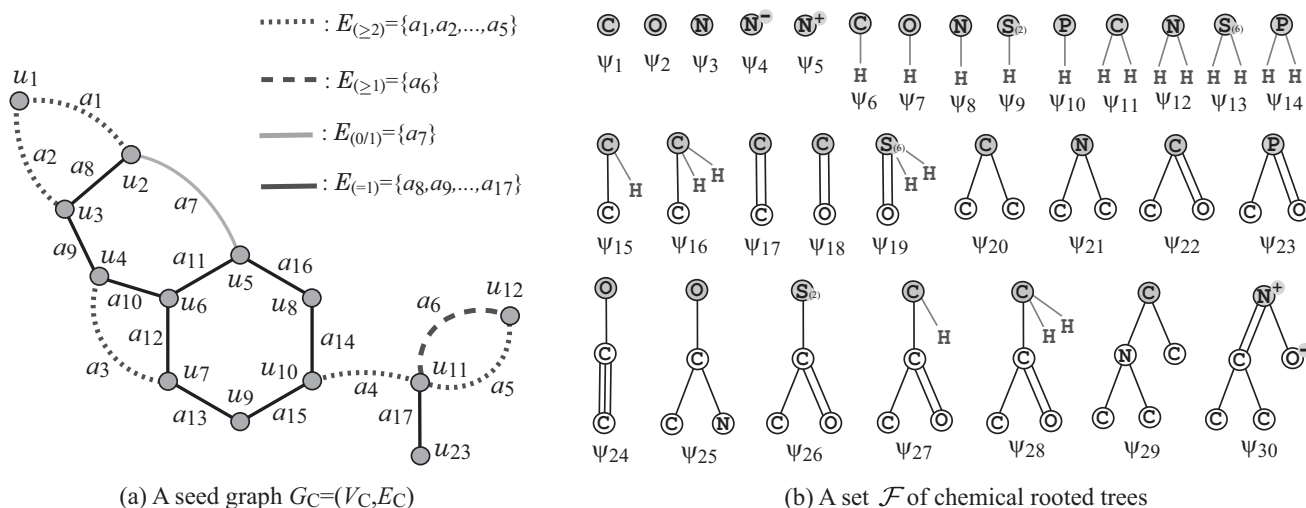


Figure 4: (a) An illustration of a seed graph G_C , where the vertices in V_C are depicted with gray circles, the edges in $E_{(\geq 2)}$ are depicted with dotted lines, the edges in $E_{(\geq 1)}$ are depicted with dashed lines, the edges in $E_{(0/1)}$ are depicted with gray bold lines and the edges in $E_{(=1)}$ are depicted with black solid lines; (b) A set $\mathcal{F} = \{\psi_1, \psi_2, \dots, \psi_{30}\} \subseteq \mathcal{F}(\mathcal{C}_\pi)$ of 30 chemical rooted trees $\psi_i, i \in [1, 30]$, where the root of each tree is depicted with a gray circle. The hydrogens attached to non-root vertices are omitted in the figure.

ψ_{19} for $\mathbb{C}[u_{15}]$, ψ_{23} for $\mathbb{C}[u_{21}]$, ψ_{24} for $\mathbb{C}[u_{24}]$, ψ_{25} for $\mathbb{C}[u_{27}]$, ψ_{26} for $\mathbb{C}[u_{23}]$, ψ_{27} for $\mathbb{C}[u_{14}]$ and ψ_{30} for $\mathbb{C}[u_{28}]$.

See Appendix C for a full description of topological specification.

4 How to Compute a Quadratic Term in an MILP

This section introduces an MILP formulation for computing the product of two descriptors in an MILP.

Given two real values x and y with $0 \leq x \leq 1$ and $0 \leq y \leq 1$, the computing process of the product $z = xy$ can be approximately formulated as the following MILP. First regard $(2^{p+1} - 1)x$ as an integer with a binary expression of $p + 1$ bits, where $x^{(j)} \in [0, 1]$ denotes the value of the j -th bit. Then compute $y \cdot x^{(j)}$ which becomes the j -th bit $z^{(j)}$ of $(2^{p+1} - 1)z$.

constants:

- x, y : reals with $0 \leq x, y \leq 1$;
- p : a positive integer;

variables:

- $z, z^{(j)}, j \in [0, p]$: reals with $0 \leq z, z^{(j)} \leq 1$;
- $x^{(j)} \in [0, 1], j \in [0, p]$: binary variables;

constraints:

$$\begin{aligned}
 \sum_{j \in [0, p]} 2^j x^{(j)} - 1 &\leq (2^{p+1} - 1)x \leq \sum_{j \in [0, p]} 2^j x^{(j)}, \\
 z^{(j)} &\leq x^{(j)}, & j \in [0, p], \\
 y - (1 - x^{(j)}) &\leq z^{(j)} \leq y + (1 - x^{(j)}), & j \in [0, p], \\
 z &= \frac{1}{2^{p+1} - 1} \sum_{j \in [0, p]} 2^j z^{(j)}. & (2)
 \end{aligned}$$

Note that the necessary number of integer variables for computing xy for one pair of x and y is p . In this paper, we set $p := 6$ in our computational experiment. The relative error by $p = 6$ in the above method is at most $\frac{1}{2^{p+1}-1} = 1/127$, which is around 0.8%.

5 Results

With our new method of choosing descriptors and formulating an MILP to treat quadratic descriptors in the two-layered model, we implemented the framework for inferring chemical graphs and conducted experiments to evaluate the computational efficiency. We executed the experiments on a PC with Processor: Core i7-9700 (3.0GHz; 4.7 GHz at the maximum) and Memory: 16 GB RAM DDR4. To construct a prediction function by LLR, MLR or ANN, we used `scikit-learn` version 1.0.2 with Python 3.8.12, MLPRegressor and ReLU activation function.

5.1 Results on the First Phase of the Framework

Chemical properties We implemented the first phase for the following 32 chemical properties of monomers and ten chemical properties of polymers.

For monomers, we used the following data sets:

biological half life (BHL), boiling point (BP), critical temperature (CT), critical pressure (CP), dissociation constants (DC), flash point in closed cup (FP), heat of combustion (HC), heat of vaporization (HV), octanol/water partition coefficient (KOW), melting point (MP), optical rotation (OPTR), refractive index of trees (RFIDT), vapor density (VD) and vapor pressure (VP), provided by HSDB from PubChem [27];
 electron density on the most positive atom (EDPA) and Kovats retention index (KOV) by M. Jalali-Heravi and M. Fatemi [28];
 entropy (ET) by P. Duchowicz et al. [29];
 heat of atomization (HA) and heat of formation (HF) by K. Roy and A. Saha [30];
 surface tension (SFT) by V. Goussard et al. [31];
 viscosity (VIS) by V. Goussard et al. [32];
 isobaric heat capacities liquid (LHCL) and isobaric heat capacities solid (LHCS) by R. Naef [33];
 lipophilicity (LP) by N. Xiao [34];
 flammable limits lower of organics (FLMLO) by S. Yuan et al. [35];
 molar refraction at 20 degree (MR) by Y. M. Ponce [36]; and
 solubility (SL) by ESOL [37],

energy of highest occupied molecular orbital (HOMO), energy of lowest unoccupied molecular orbital (LUMO), the energy difference between HOMO and LUMO (GAP), isotropic polarizability (ALPHA), heat capacity at 298.15K (Cv), internal energy at 0K (U0) and electric dipole moment (MU) provided by ESOL [37], where the properties from HOMO to MU are based on a common data set QM9.

The data set QM9 contains more than 130,000 compounds. In our experiment, we use a set of 1,000 compounds randomly selected from the data set. For property Hv, we remove the chemical compound with CID=7947 as an outlier from the original data set.

For polymers, we used the following data provided by J. Bicerano [38]: experimental amorphous density (AMD), characteristic ratio (CHAR), dielectric constant (DIEC), dissipation factor (DISF), heat capacity in liquid (HCL), heat capacity in solid (HCS), mol volume (MLV), permittivity (PRM), refractive index of polymers (RFIDP) and glass transition (TG), where we excluded from our test data set every polymer whose chemical formula could not be found by its name in the book [38]. We remark that the previous learning experiments for $\pi \in \{\text{CHAR}, \text{RFIDP}\}$ based on the two-layered model due to Azam et al. [23] and Zhu et al. [26] excluded some number of polymers as outliers. In our experiments, we do not exclude any polymer from the original data set as outliers for these properties.

Setting data sets For each property π , we first select a set Λ of chemical elements and then collect a data set \mathcal{C}_π on chemical graphs over the set Λ of chemical elements. To construct the data set \mathcal{C}_π , we eliminated chemical compounds that do not satisfy one of the following: the graph is connected, the number of carbon atoms is at least four, and the number of non-hydrogen neighbors of each atom is at most 4.

We set a branch-parameter ρ to be 2, introduce linear descriptors defined by the two-layered graph in the chemical model without suppressing hydrogen and use the set $D_\pi^{(1)} \cup D_\pi^{(2)}$ of linear and quadratic descriptors (see Appendix A for the details). We normalize the range of each linear descriptor and the range $\{t \in \mathbb{R} \mid \underline{a} \leq t \leq \bar{a}\}$ of property values $a(\mathbb{C}), \mathbb{C} \in \mathcal{C}_\pi$.

We compare the following four methods of constructing a prediction function.

- (i) **LLR**: use Lasso linear regression on the set the $D_\pi^{(1)}$ of linear descriptors (see [21] for the detail of the implementation);
- (ii) **ANN**: use ANN on the set the $D_\pi^{(1)}$ of linear descriptors (see [21] for the detail of the implementation);
- (iii) **ALR**: use adjustive linear regression on the set the $D_\pi^{(1)}$ of linear descriptors (see [26] for the detail of the implementation); and
- (iv) **R-MLR**: apply our method (see Appendix B) of reducing descriptors to the set $D_\pi^{(1)} \cup D_\pi^{(2)}$ of linear and quadratic descriptors and use multi-linear regression for the resulting set of descriptors.

Among the above properties, we found that the median of test coefficient of determination R^2 of the prediction function constructed by LLR [21] or ALR [26] exceeds 0.98 for the following

Table 1: Results of setting data sets for monomers.

π	Λ	$ \mathcal{C}_\pi $	\underline{n}, \bar{n}	\underline{a}, \bar{a}	$ \Gamma $	$ \mathcal{F} $	K_1
BHL	Λ_7	514	5, 36	0.03, 732.99	26	101	166
BP	Λ_2	370	4, 67	-11.7, 470.0	22	130	184
BP	Λ_7	444	4, 67	-11.7, 470.0	26	163	230
CP	Λ_5	131	4, 63	$4.7 \times 10^{-6}, 5.52$	8	79	119
CT	Λ_2	125	4, 63	56.1, 3607.5	8	76	113
CT	Λ_5	132	4, 63	56.1, 3607.5	8	81	121
DC	Λ_2	141	5, 44	0.5, 17.11	20	62	111
DC	Λ_7	161	5, 44	0.5, 17.11	25	69	130
ET	Λ_7	17	5, 12	64.34, 96.21	5	17	53
FP	Λ_2	368	4, 67	-82.99, 300.0	20	131	183
FP	Λ_7	424	4, 67	-82.99, 300.0	25	161	229
FLMLO	Λ_{16}	1046	1, 49	0.185, 4.3	34	282	376
HV	Λ_2	94	4, 16	19.12, 210.3	12	63	105
KOV	Λ_1	52	11, 16	1422.0, 1919.0	9	33	64
KOW	Λ_2	684	4, 58	-7.5, 15.6	25	166	223
KOW	Λ_8	899	4, 69	-7.5, 15.6	37	219	303
LP	Λ_2	615	6, 60	-3.62, 6.84	32	116	186
LP	Λ_8	936	6, 74	-3.62, 6.84	44	136	231
MP	Λ_2	467	4, 122	-185.33, 300.0	23	142	197
MP	Λ_8	577	4, 122	-185.33, 300.0	32	176	255
OPTR	Λ_2	147	5, 44	-117.0, 165.0	21	55	107
OPTR	Λ_4	157	5, 69	-117.0, 165.0	25	62	123
RfidT	Λ_{10}	191	4, 26	0.919, 1.613	17	115	168
SL	Λ_2	673	4, 55	-9.332, 1.11	27	154	217
SL	Λ_8	915	4, 55	-11.6, 1.11	42	207	300
SFT	Λ_3	247	5, 33	12.3, 45.1	11	91	128
VIS	Λ_3	282	5, 36	-0.64, 1.63	12	88	126
HOMO	Λ_9	977	6, 9	-0.3335, -0.1583	59	190	297
LUMO	Λ_9	977	6, 9	-0.1144, 0.1026	59	190	297
GAP	Λ_9	977	6, 9	0.1324, 0.4117	59	190	297
ALPHA	Λ_9	977	6, 9	50.9, 99.6	59	190	297
CV	Λ_9	977	6, 9	19.2, 44.0	59	190	297
MU	Λ_9	977	6, 9	0.04, 6.897	59	190	297

nine properties of monomers (resp., three properties of polymers): EDPA, HC, HA, HF, LHCL, LHCS, MR, VD and U0 (resp., HCL, HCS and MLV). We excluded the above properties in the following experiment, and used the rest of 23 chemical properties of monomers and seven chemical properties of polymers to compare the four methods (i)-(iv).

Table 2: Results of setting data sets for polymers.

π	Λ	$ \mathcal{C}_\pi $	\underline{n}, \bar{n}	\underline{a}, \bar{a}	$ \Gamma $	$ \mathcal{F} $	K_1
AMD	Λ_2	86	4, 45	0.838, 1.34	16	25	83
AMD	Λ_{13}	93	4, 45	0.838, 1.45	18	30	94
CHAR	Λ_2	30	4, 18	3.7, 15.9	15	17	68
CHAR	Λ_{12}	32	4, 18	3.7, 15.9	15	18	71
CHAR	Λ_6	35	4, 18	3.7, 15.9	18	21	83
DEIC	Λ_{12}	36	4, 22	2.13, 3.4	11	18	67
DISF	Λ_{13}	132	4, 45	$7 \times 10^{-5}, 0.07$	15	18	78
PRM	Λ_2	112	4, 45	2.23, 4.91	14	15	69
PRM	Λ_{13}	132	4, 45	2.23, 4.91	15	18	78
RFIDP	Λ_{11}	92	4, 29	0.4899, 1.683	15	35	96
RFIDP	Λ_{14}	125	4, 29	0.4899, 1.683	19	50	124
RFIDP	Λ_{15}	135	4, 29	0.4899, 1.71	23	56	144
TG	Λ_2	204	4, 58	171, 673	19	36	101
TG	Λ_7	232	4, 58	171, 673	21	43	118

Tables 1 and 2 show the size and range of data sets that we prepared for each chemical property to construct a prediction function, where we denote the following:

- π : the name of a chemical property used in the experiment.
- Λ : a set of selected elements used in the data set \mathcal{C}_π ; Λ is one of the following 19 sets:
 $\Lambda_1 = \{\text{H, C, O}\}$; $\Lambda_2 = \{\text{H, C, O, N}\}$; $\Lambda_3 = \{\text{H, C, O, Si}_{(4)}\}$; $\Lambda_4 = \{\text{H, C, O, N, S}_{(2)}, \text{F}\}$;
 $\Lambda_5 = \{\text{H, C, O, N, Cl, Pb}\}$; $\Lambda_6 = \{\text{H, C, O, N, Si}_{(4)}, \text{Cl, Br}\}$; $\Lambda_7 = \{\text{H, C, O, N, S}_{(2)}, \text{S}_{(6)}, \text{Cl}\}$;
 $\Lambda_8 = \{\text{H, C, O, N, S}_{(2)}, \text{S}_{(4)}, \text{S}_{(6)}, \text{Cl}\}$; $\Lambda_9 = \{\text{H, C}_{(2)}, \text{C}_{(3)}, \text{C}_{(4)}, \text{C}_{(5)}, \text{O, N}_{(1)}, \text{N}_{(2)}, \text{N}_{(3)}, \text{F}\}$;
 $\Lambda_{10} = \{\text{H, C, O, N, P}_{(2)}, \text{P}_{(5)}, \text{Cl}\}$; $\Lambda_{11} = \{\text{H, C, O}_{(1)}, \text{O}_{(2)}, \text{N}\}$; $\Lambda_{12} = \{\text{H, C, O, N, Cl}\}$;
 $\Lambda_{13} = \{\text{H, C, O, N, Cl, S}_{(2)}\}$; $\Lambda_{14} = \{\text{H, C, O}_{(1)}, \text{O}_{(2)}, \text{N, Cl, Si}_{(4)}, \text{F}\}$;
 $\Lambda_{15} = \{\text{H, C, O}_{(1)}, \text{O}_{(2)}, \text{N, Si}_{(4)}, \text{Cl, F, S}_{(2)}, \text{S}_{(6)}, \text{Br}\}$;
 $\Lambda_{16} = \{\text{H, C, O}_{(2)}, \text{N, Cl, P}_{(3)}, \text{P}_{(5)}, \text{S}_{(2)}, \text{S}_{(4)}, \text{S}_{(6)}, \text{Si}_{(4)}, \text{Br, I}\}$, where $\mathbf{a}_{(i)}$ for a chemical element \mathbf{a} and an integer $i \geq 1$ means that a chemical element \mathbf{a} with valence i .
- $|\mathcal{C}_\pi|$: the size of data set \mathcal{C}_π over Λ for the property π .
- \underline{n}, \bar{n} : the minimum and maximum values of the number $n(\mathbb{C})$ of non-hydrogen atoms in the compounds \mathbb{C} in \mathcal{C}_π .
- \underline{a}, \bar{a} : the minimum and maximum values of $a(\mathbb{C})$ for π over the compounds \mathbb{C} in \mathcal{C}_π .
- $|\Gamma|$: the number of different edge-configurations of interior-edges over the compounds in \mathcal{C}_π .
- $|\mathcal{F}|$: the number of non-isomorphic chemical rooted trees in the set of all 2-fringe-trees in the compounds in \mathcal{C}_π .
- K_1 : the size $|D_\pi^{(1)}|$ of a set $D_\pi^{(1)}$ of linear descriptors, where $|D_\pi^{(2)}| = (3(K_1)^2 + K_1)/2$ holds.

Constructing prediction functions For each chemical property π , we construct a prediction function by one of the four methods (i)-(iv).

For methods (i)-(iii), we used the same implementation due to Zhu et al. [21, 26] and omit the

details.

In method (iv), we use our new procedures LLR-Reduce and Select-Des-set for reducing the number of descriptors (see Appendix B for the details). Method (iv) for property π is implemented as follows. If π is a monomer property and $|D_\pi^{(1)} \cup D_\pi^{(2)}| > 5000$ then first execute LLR-Reduce($\mathcal{C}_\pi, D_\pi^{(1)} \cup D_\pi^{(2)}$) to find a subset \tilde{D} of $D_\pi^{(1)} \cup D_\pi^{(2)}$ with 5000 descriptors. Otherwise set $\tilde{D} := D_\pi^{(1)} \cup D_\pi^{(2)}$. Next execute Select-Des-set($\mathcal{C}_\pi, \tilde{D}$) to obtain a subset D^* of \tilde{D} . Construct a prediction function by MLR on the selected descriptor set D^* .

Tables 3 and 4 show the results on constructing prediction functions, where we denote the following:

- π : the name of a chemical property used in the experiment.
- Λ : the set of elements selected from the data set \mathcal{C}_π .
- LLR: the median of test R^2 in ten 5-fold cross-validations for prediction functions constructed by method (i).
- ANN: the median of test R^2 in ten 5-fold cross-validations for prediction functions constructed by method (ii).
- ALR: the median of test R^2 in ten 5-fold cross-validations for prediction functions constructed by method (iii).
- R-MLR: the median of test R^2 in ten 5-fold cross-validations for prediction functions constructed by method (iv).
- the score of LLR, ANN, ALR or R-MLR marked with “*” indicates the best performance among the four methods for the property π ;
- K_1^*, K_2^* : the numbers K_1^* and K_2^* of linear and quadratic descriptors, respectively in the set D^* selected by our method (iv) from the set $D_\pi^{(1)} \cup D_\pi^{(2)}$ before a prediction function is constructed by MLR in (iv).

The running time of choosing a descriptor set D^* in method (iv) was around from 80 to 4×10^4 seconds and the time for constructing a prediction function to D^* is around 0.03 to 0.46 second.

There are 47 instances for constructing prediction functions in Tables 3 and 4. From these tables, we observe that method (iv) using quadratic descriptors performs better than methods (i)-(iii) with linear descriptors only in 43 out of the 47 instances. The averages of the median test R^2 of the method (i)-(iv) over the 47 instances are 0.634, 0.733, 0.764 and 0.913, respectively. In particular, method (iv) considerably improved the performance for $\pi \in \{\text{BP, CP, DC, ET, FP, HV, KOV, LP, RFI DT, GAP, CHAR, DISF, PRM, RFI DP}\}$. We also see that most descriptors in the resulting descriptor set D^* in R-MLR are quadratic.

5.2 Results on the Second Phase of the Framework

To execute the second phase, we used a set of seven instances $I_a, I_b^i, i \in [1, 4], I_c$ and I_d based on the seed graphs prepared by Zhu et al. [21]. We here present their seed graphs G_C (see Appendix C for the details of I_a and Appendix D for the details of $I_b^i, i \in [1, 4], I_c$ and I_d).

The seed graph G_C of I_a is given by the graph in Figure 4(a). The seed graph G_C^1 of I_b^1 (resp., $G_C^i, i = 2, 3, 4$ of $I_b^i, i = 2, 3, 4$) is illustrated in Figure 5.

Instance I_c has been introduced in order to infer a chemical graph \mathbb{C}^\dagger such that

- a core part of \mathbb{C}^\dagger is equal to that of chemical graph \mathbb{C}_A : CID 24822711 in Figure 6(a)

Table 3: Results of constructing prediction functions for monomers.

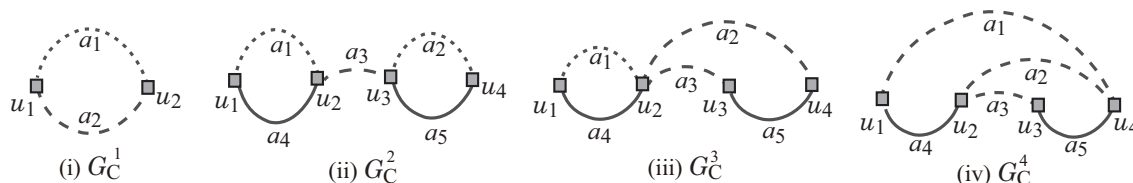
π	Λ	LLR	ANN	ALR	R-MLR	K_1^*, K_2^*
BHL	Λ_7	0.483	0.622	0.265	*0.659	0, 27
BP	Λ_2	0.599	0.765	0.816	*0.935	1, 59
BP	Λ_7	0.663	0.720	0.832	*0.899	0, 38
CP	Λ_5	0.555	0.727	0.690	*0.841	0, 67
CT	Λ_2	0.037	0.357	0.900	*0.937	1, 47
CT	Λ_5	0.048	0.357	*0.895	0.860	0, 13
DC	Λ_2	0.489	0.651	0.488	*0.908	0, 58
DC	Λ_7	0.574	0.622	0.602	*0.829	0, 26
ET	Λ_7	0.132	0.479	0.464	*0.996	0, 13
FP	Λ_2	0.589	0.746	0.719	*0.899	0, 42
FP	Λ_7	0.571	0.745	0.684	*0.846	0, 32
FLMLO	Λ_{16}	0.819	0.928	0.604	*0.949	0, 77
HV	Λ_2	0.864	0.778	0.816	*0.970	0, 22
KOV	Λ_1	0.677	0.727	0.838	*0.953	2, 19
KOW	Λ_2	0.953	0.952	0.964	*0.967	0, 55
KOW	Λ_8	0.927	0.937	*0.952	0.950	0, 64
LP	Λ_2	0.856	0.867	0.844	*0.928	0, 89
LP	Λ_8	0.840	0.859	0.807	*0.914	0, 109
MP	Λ_2	0.810	0.800	0.831	*0.873	0, 51
MP	Λ_8	0.810	0.820	0.807	*0.898	0, 58
OPTR	Λ_2	0.825	0.918	0.876	*0.970	0, 85
OPTR	Λ_4	0.825	0.878	0.870	*0.970	0, 69
RFIDT	Λ_{10}	0.000	0.453	0.425	*0.775	0, 43
SL	Λ_2	0.808	0.848	0.784	*0.894	0, 82
SL	Λ_8	0.808	0.861	0.828	*0.897	0, 74
SFT	Λ_3	0.927	0.859	0.847	*0.941	0, 36
VIS	Λ_3	0.893	0.929	0.911	*0.973	0, 43
HOMO	Λ_9	*0.841	0.689	0.689	0.804	0, 87
LUMO	Λ_9	0.841	0.860	0.833	*0.920	0, 102
GAP	Λ_9	0.784	0.795	0.755	*0.876	0, 83
ALPHA	Λ_9	0.961	0.888	0.953	*0.980	0, 104
CV	Λ_9	0.970	0.911	0.966	*0.978	0, 83
MU	Λ_9	0.367	0.409	0.403	*0.645	0, 112

(where the seed graph G_C of I_c is indicated by the shaded area in Figure 6(a)).

- the frequency of each edge-configuration in the non-core of \mathbb{C}^\dagger is equal to that of chemical graph \mathbb{C}_B : CID 59170444 in Figure 6(b).

Table 4: Results of constructing prediction functions for polymers.

π	Λ	LLR	ANN	ALR	R-MLR	K_1^*, K_2^*
AMD	Λ_2	0.914	0.885	*0.933	0.906	0, 5
AMD	Λ_{13}	0.918	0.824	0.917	*0.953	0, 6
CHAR	Λ_2	0.210	0.642	0.863	*0.938	0, 10
CHAR	Λ_{12}	0.088	0.640	0.835	*0.924	0, 9
CHAR	Λ_6	-0.073	0.527	0.766	*0.950	0, 12
DEIC	Λ_{12}	0.761	0.641	0.918	*0.956	3, 41
DISF	Λ_{13}	0.623	0.801	0.308	*0.906	1, 23
PRM	Λ_2	0.801	0.801	0.505	*0.967	0, 26
PRM	Λ_{13}	0.784	0.735	0.489	*0.977	0, 34
RFIDP	Λ_{11}	0.104	0.423	0.853	*0.962	2, 52
RFIDP	Λ_{14}	0.373	0.560	0.848	*0.953	2, 43
RFIDP	Λ_{15}	0.346	0.492	0.883	*0.947	5, 53
TG	Λ_2	0.902	0.883	0.923	*0.958	1, 33
TG	Λ_7	0.894	0.860	0.927	*0.957	0, 32

Figure 5: (i) Seed graph G_C^1 for I_b^1 and I_d ; (ii) Seed graph G_C^2 for I_b^2 ; (iii) Seed graph G_C^3 for I_b^3 ; (iv) Seed graph G_C^4 for I_b^4 .

Instance I_d has been introduced in order to infer a chemical graph \mathbb{C}^\dagger such that

- \mathbb{C}^\dagger is monocyclic (where the seed graph of I_d is given by G_C^1 in Figure 5(i)); and
- the frequency vector of edge-configurations in \mathbb{C}^\dagger is a vector obtained by merging those of chemical graphs \mathbb{C}_A : CID 10076784 and \mathbb{C}_B : CID 44340250 in Figure 6(c) and (d), respectively.

Solving an MILP for the inverse problem. We executed the stage of solving an MILP to infer a chemical graph for two properties $\pi \in \{\text{BP}, \text{DC}\}$.

For the MILP formulation $\mathcal{M}_{f,\eta,\sigma}$, we use the prediction function η for each $\pi \in \{\text{BP}, \text{DC}\}$ by method (iv), R-MLR that attained the median test R^2 in Table 3. To solve an MILP with the formulation, we used CPLEX version 12.10. Tables 5 and 6 show the computational results of the experiment in this stage for the two properties, where we denote the following:

- n_{LB} : a lower bound on the number of non-hydrogen atoms in a chemical graph \mathbb{C} to be inferred;
- $\underline{y}^*, \bar{y}^*$: lower and upper bounds $\underline{y}^*, \bar{y}^* \in \mathbb{R}$ on the value $a(\mathbb{C})$ of a chemical graph \mathbb{C} to be inferred;
- $\#v$ (resp., $\#c$): the number of variables (resp., constraints) in the MILP;

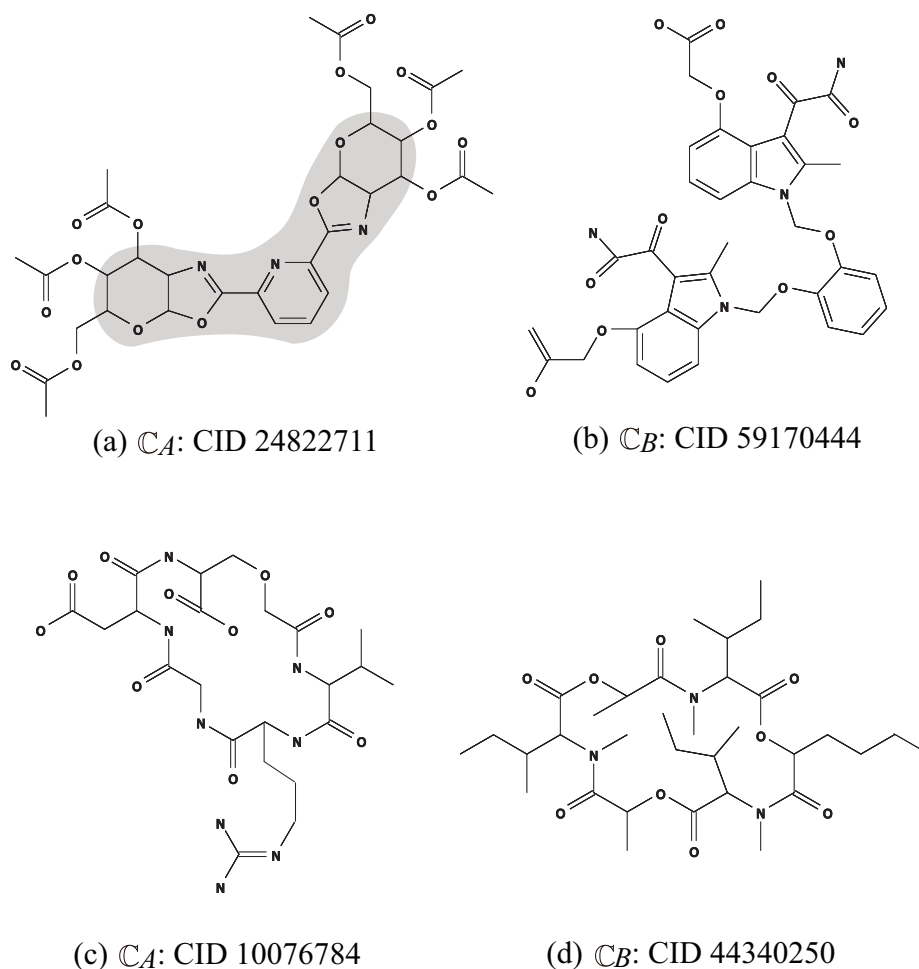


Figure 6: An illustration of chemical compounds for instances I_c and I_d : (a) \mathbb{C}_A : CID 24822711; (b) \mathbb{C}_B : CID 59170444; (c) \mathbb{C}_A : CID 10076784; (d) \mathbb{C}_B : CID 44340250, where hydrogens are omitted.

- I-time: the time (sec.) to solve the MILP;
- n : the number $n(\mathbb{C}^\dagger)$ of non-hydrogen atoms in the chemical graph \mathbb{C}^\dagger inferred by solving the MILP;
- n^{int} : the number $n^{\text{int}}(\mathbb{C}^\dagger)$ of interior-vertices in the chemical graph \mathbb{C}^\dagger ; and
- η : the predicted property value $\eta(f(\mathbb{C}^\dagger))$ of the chemical graph \mathbb{C}^\dagger .

Figure 7(a) illustrates the chemical graph \mathbb{C}^\dagger inferred from I_c with $(\underline{y}^*, \overline{y}^*) = (340, 350)$ of BP in Table 5.

Figure 7(b) (resp., Figure 7(c)) illustrates the chemical graph \mathbb{C}^\dagger inferred from I_a with $(\underline{y}^*, \overline{y}^*) = (0.55, 0.60)$ (resp., I_d with $(\underline{y}^*, \overline{y}^*) = (3.15, 3.20)$) of DC in Table 6.

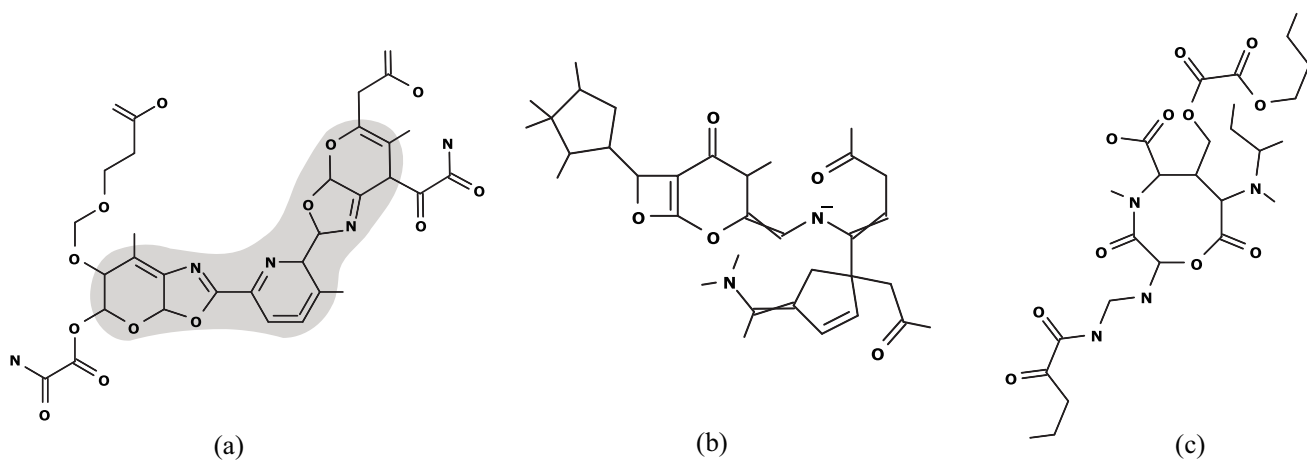
In this experiment, we prepared several different types of instances: instances I_a and I_c have restricted seed graphs, the other instances have abstract seed graphs and instances I_c and I_d have restricted set of fringe-trees. From Tables 5 and 6, we observe that an instance with a large number of variables and constraints takes more running time than those with a smaller size in general. All instances in this experiment are solved in a few seconds to around 60 seconds with our MILP

Table 5: Results of inferring a chemical graph \mathbb{C}^\dagger and generating recombination solutions for BP with Λ_7 .

inst.	n_{LB}	$\underline{y}^*, \overline{y}^*$	#v	#c	I-time	n	n^{int}	η	D-time	C-LB	#C
I_a	30	225, 235	10502	10240	4.29	49	26	233.92	0.072	3	3
I_b^1	35	285, 295	10507	7793	2.27	35	10	286.52	0.034	6	6
I_b^2	45	365, 375	13000	10913	11.9	49	25	370.70	0.14	3202	100
I_b^3	45	305, 315	12788	10920	7.07	48	25	309.39	0.22	6304	100
I_b^4	45	260, 270	12576	10928	10.7	49	27	266.26	0.17	376	100
I_c	50	340, 350	7515	8270	0.867	50	33	344.98	0.019	2	2
I_d	40	320, 330	6135	7773	8.22	45	23	329.85	8.3	6733440	100

Table 6: Results of inferring a chemical graph \mathbb{C}^\dagger and generating recombination solutions for DC with Λ_7 .

inst.	n_{LB}	$\underline{y}^*, \overline{y}^*$	#v	#c	I-time	n	n^{int}	η	D-time	C-LB	#C
I_a	30	0.55, 0.60	10194	9787	3.91	41	25	0.558	0.069	2	2
I_b^1	35	1.10, 1.15	10415	7368	4.73	35	11	1.104	0.10	16	16
I_b^2	45	6.00, 6.05	12976	10481	57.4	45	25	6.04	0.12	2040	100
I_b^3	45	1.45, 1.50	2767	10488	39.7	49	26	1.488	0.28	21600	100
I_b^4	45	6.10, 6.15	12558	10494	26.4	46	25	6.10	0.027	2	2
I_c	50	12.35, 12.40	7207	7819	1.75	50	34	12.38	0.020	2	2
I_d	40	3.15, 3.20	5827	7325	14.9	41	23	3.199	0.079	18952	100

Figure 7: (a) \mathbb{C}^\dagger with $\eta(f(\mathbb{C}^\dagger)) = 344.98$ inferred from I_c with $(\underline{y}^*, \overline{y}^*) = (340, 350)$ of BP; (b) \mathbb{C}^\dagger with $\eta(f(\mathbb{C}^\dagger)) = 0.558$ inferred from I_a with $(\underline{y}^*, \overline{y}^*) = (0.55, 0.60)$ of DC; and (c) \mathbb{C}^\dagger with $\eta(f(\mathbb{C}^\dagger)) = 3.199$ inferred from I_d with $(\underline{y}^*, \overline{y}^*) = (3.15, 3.20)$ of DC.

formulation.

Generating recombination solutions. Let \mathbb{C}^\dagger be a chemical graph obtained by solving the MILP $\mathcal{M}_{f,\eta,\sigma}$ for the inverse problem. We here execute a stage of generating recombination solutions $\mathbb{C}^* \in \mathcal{G}_\sigma$ of \mathbb{C}^\dagger such that $f(\mathbb{C}^*) = x^* = f(\mathbb{C}^\dagger)$.

We execute an algorithm for generating chemical isomers of \mathbb{C}^\dagger up to 100 when the number of all chemical isomers exceeds 100. For this, we use a dynamic programming algorithm [21]. The algorithm first decomposes \mathbb{C}^\dagger into a set of acyclic chemical graphs, next replaces each acyclic chemical graph T with another acyclic chemical graph T' that admits the same feature vector as that of T and finally assembles the resulting acyclic chemical graphs into a chemical isomer \mathbb{C}^* of \mathbb{C}^\dagger . The algorithm can compute a lower bound on the total number of all chemical isomers \mathbb{C}^\dagger without generating all of them.

Tables 5 and 6 show the computational results of the experiment in this stage for the two properties $\pi \in \{\text{BP}, \text{DC}\}$, where we denote the following:

- D-time: the running time (sec.) to execute the dynamic programming algorithm to compute a lower bound on the number of all chemical isomers \mathbb{C}^* of \mathbb{C}^\dagger and generate all (or up to 100) chemical isomers \mathbb{C}^* ;
- C-LB: a lower bound on the number of all chemical isomers \mathbb{C}^* of \mathbb{C}^\dagger ; and
- #C: the number of all (or up to 100) chemical isomers \mathbb{C}^* of \mathbb{C}^\dagger generated in this stage.

From Tables 5 and 6, we observe the running time and the number of generated recombination solutions in this stage.

The chemical graph \mathbb{C}^\dagger in I_b^2 , I_b^3 and I_d admits a large number of chemical isomers \mathbb{C}^* in some cases, where a lower bound C-LB on the number of chemical isomers is derived without generating all of them. For the other instances, the running time for generating up to 100 target chemical graphs in this stage is less than 0.03 second. For some chemical graph \mathbb{C}^\dagger , the number of chemical isomers found by our algorithm was small. This is because some of acyclic chemical graphs in the decomposition of \mathbb{C}^\dagger has no alternative acyclic chemical graph other than the original one.

Generating neighbor solutions. Let \mathbb{C}^\dagger be a chemical graph obtained by solving the MILP $\mathcal{M}_{f,\eta,\sigma}$ for the inverse problem. We executed a stage of generating neighbor solutions of \mathbb{C}^\dagger .

We select an MILP for the inverse problem with a prediction function η such that a solution \mathbb{C}^\dagger of the MILP admits only two isomers \mathbb{C}^* in the stage of generating recombination solutions; i.e., instance I_c for property BP with Λ_7 and instances I_a , I_b^4 and I_c for property DC with Λ_7 .

In this experiment, we add to the MILP $\mathcal{M}_{f,\eta,\sigma}$ an additional set Θ of two linear constraints on linear and quadratic descriptors as follows. For the two constraints, we use the prediction functions η_π constructed by R-MLR for properties $\pi \in \{\text{LP}, \text{SL}\}$ with Λ_8 in Table 3.

Let D_π^* denote the set of descriptors selected in the construction of prediction function for properties $\pi \in \{\text{BP}, \text{DC}\}$ with Λ_7 and $\pi \in \{\text{LP}, \text{SL}\}$ with Λ_8 in Table 3 and let D_π^{union} , $\pi \in \{\text{BP}, \text{DC}\}$ denote the union $D_\pi^* \cup D_{\text{LP}}^* \cup D_{\text{SL}}^*$. We regard each of η_{LP} and η_{SL} as a function from $\mathbb{R}^{|D_\pi^{\text{union}}|}$ to \mathbb{R} for $\pi \in \{\text{BP}, \text{DC}\}$. We set $p_{\text{dim}} := 2$ and let Θ consist of two linear constraints $\theta_1 := \eta_{\text{LP}}$ and $\theta_2 := \eta_{\text{SL}}$. We set $\delta := 0.1$ or 0.05 which defines a two-dimensional grid space where \mathbb{C}^\dagger is mapped to the origin (see [23] for the detail on the neighbors). We choose a set N_0 of 48 neighbors of the origin \mathbb{C}^\dagger in the grid search space. For each instance, we check the feasibility of neighbors in N_0 in a non-decreasing order of the distance between the neighbor and the origin. For each feasible

neighbor $z \in N_0$, output a feasible solution \mathbb{C}_z^\dagger of the augmented MILP instance. We set a time limit for checking the feasibility of a neighbor to be 300 seconds, and we skip a neighbor when the corresponding MILP is not solved within the time limit. We also ignore any neighbor $z \in N_0$ without testing the feasibility of z if we find an infeasible neighbor $z' \in N_0$ such that z' is closer to the origin than z is.

Table 7 shows the computational results of the experiment for the three instances, where we denote the following:

- (inst., π): topological specification I and property π ;
- n : the number of non-hydrogen atoms in the tested instance;
- δ : the size of a sub-region in the grid search space;
- #sol: the number of new chemical graphs obtained from the neighbor set N_0 ;
- #infs: the number of neighbors in N_0 that are found to be infeasible during the search procedure;
- #ign: the number of neighbors in N_0 that are ignored during the search procedure;
- #TO: the number of neighbors in N_0 such that the time for feasibility check exceeds the time limit of 300 seconds during the search procedure.

Table 7: Results of generating neighbor solutions of \mathbb{C}^\dagger .

(inst., π)	n	δ	#sol	#infs	#ign	#TO
(I_c ,BP)	50	0.1	5	1	3	39
(I_a ,DC)	30	0.1	40	1	0	7
(I_b^4 ,DC)	45	0.1	2	0	0	46
(I_c ,DC)	40	0.05	0	0	0	48

The branch-and-bound method for solving an MILP sometimes takes an extremely large execution time for the same size of instances. We introduce a time limit to bound an entire running time to skip such instances during an execution of testing the feasibility of neighbors in N_0 . From Table 7, we observe that some number of neighbor solutions of the solution \mathbb{C}^\dagger to the MILP $\mathcal{M}_{f,\eta,\sigma}$ could be generated for each of the four instances.

6 Concluding Remarks

In the framework of inferring chemical graphs, the descriptors of a prediction function were mainly defined to be the frequencies of local graph structures in the two-layered model and such definition was important to derive a compact MILP formulation for inferring a desired chemical graph. To improve the performance of prediction functions in the framework, this paper introduced a multiple of two of these descriptors as a new descriptor and examined the effectiveness of the new set of descriptors. For this, we designed a method for reducing the size of a descriptor set not to lose the learning performance in constructing prediction functions and gave a compact formulation to compute a product of two values in an MILP. From the results of our computational experiments, we observe that a prediction function constructed by our new method performs considerably better

than the previous prediction functions for many chemical properties. We also found that the modified MILP in the second phase of the framework still can infer a chemical graph with around 50 non-hydrogen atoms.

References

- [1] Lo, Y-C., Rensi, S. E., Torng, W., Altman, R. B.: Machine learning in chemoinformatics and drug discovery. *Drug Discovery Today* 23, 1538–1546 (2018)
- [2] Tetko, I. V., Engkvist, O.: From big data to artificial intelligence: chemoinformatics meets new challenges. *J. Cheminformatics* 12, 74 (2020)
- [3] Cherkasov, A., Muratov, E. N., Fourches, D., Varnek, A., Baskin, I. I., Cronin, M., Dearden, J., Gramatica, P., Martin, Y. C., Todeschini, R., et al. QSAR modeling: where have you been? Where are you going to? *J. Med. Chem.* 57, 4977–5010 (2014)
- [4] Miyao, T., Kaneko, H., Funatsu, K.: Inverse QSPR/QSAR analysis for chemical structure generation (from y to x). *J. Chem. Inf. Model.* 56, 286–299 (2016)
- [5] Ikebata, H., Hongo, K., Isomura, T., Maezono, R., Yoshida, R.: Bayesian molecular design with a chemical language model. *J. Comput. Aided Mol. Des.* 31, 379–391 (2017)
- [6] Rupakheti, C., Virshup, A., Yang, W., Beratan, D. N.: Strategy to discover diverse optimal molecules in the small molecule universe. *J. Chem. Inf. Model.* 55, 529–537 (2015)
- [7] Ghasemi, F., Mehridehnavi, A., Pérez-Garrido, A., Pérez-Sánchez, H.: Neural network and deep-learning algorithms used in QSAR studies: merits and drawbacks. *Drug Discovery Today* 23, 1784–1790 (2018)
- [8] Kim, J., Park, S., Min, D., Kim, W.: Comprehensive survey of recent drug discovery using deep learning. *Int. J. Molecular Science* 22(18), 9983 (2022)
- [9] Bohacek, R. S., McMartin, C., Guida, W. C.: The art and practice of structure-based drug design: A molecular modeling perspective. *Med. Res. Rev.* 16, 3–50 (1996)
- [10] Akutsu, T., Fukagawa, D., Jansson, J., Sadakane, K.: Inferring a graph from path frequency. *Discrete Appl. Math.* 160, 10-11, 1416–1428 (2012)
- [11] Kipf, T. N., Welling, M.: Semi-supervised classification with graph convolutional networks. [arXiv:1609.02907](https://arxiv.org/abs/1609.02907) (2016)
- [12] Xiong, J., Xiong, Z., Chen, K., Jiang, H., Zheng, M.: Graph neural networks for automated de novo drug design. *Drug Discovery Today* 26, 1382–1393 (2022)
- [13] Segler, M. H. S., Kogej, T., Tyrchan, C., Waller, M. P.: Generating focused molecule libraries for drug discovery with recurrent neural networks. *ACS Cent. Sci.* 4, 120–131 (2017)

- [14] Yang, X., Zhang, J., Yoshizoe, K., Terayama, K., Tsuda, K.: ChemTS: an efficient python library for de novo molecular generation. *STAM* 18, 972–976 (2017)
- [15] Gómez-Bombarelli, R., Wei, J. N., Duvenaud, D., Hernández-Lobato, J. M., Sánchez-Lengeling, B., Sheberla, D., Aguilera-Iparraguirre, J., Hirzel, T. D., Adams, R. P., Aspuru-Guzik, A.: Automatic chemical design using a data-driven continuous representation of molecules. *ACS Cent. Sci.* 4, 268–276 (2018)
- [16] Kusner, M. J., Paige, B., Hernández-Lobato, J. M.: Grammar variational autoencoder. *Proc. of the 34th International Conference on Machine Learning-Volume 70, 1945–1954* (2017)
- [17] De Cao, N., Kipf, T.: MolGAN: An implicit generative model for small molecular graphs. *arXiv:1805.11973* (2018)
- [18] Madhawa, K., Ishiguro, K., Nakago, K., Abe, M.: GraphNVP: an invertible flow model for generating molecular graphs. *arXiv:1905.11600* (2019)
- [19] Shi, C., Xu, M., Zhu, Z., Zhang, W., Zhang, M., Tang, J.: GraphAF: a flow-based autoregressive model for molecular graph generation. *arXiv:2001.09382* (2020)
- [20] Shi, Y., Zhu, J., Azam, N. A., Haraguchi, K., Zhao, L., Nagamochi, H., Akutsu, T.: An inverse QSAR method based on a two-layered model and integer programming. *International Journal of Molecular Sciences* 22, 2847 (2021)
- [21] Zhu, J., Azam, N. A., Haraguchi, K., Zhao, L., Nagamochi, H., Akutsu, T.: A method for molecular design based on linear regression and integer programming. *12th International Conference on Bioscience, Biochemistry and Bioinformatics, Tokyo, Japan, January 7-10, #TJ0002, 21–28* (2022)
- [22] Ido, R., Cao, S., Zhu, J., Azam, N. A., Haraguchi, K., Zhao, L., Nagamochi, H., Akutsu, T.: A method for inferring polymers based on linear regression and integer programming. *The 20th Asia Pacific Bioinformatics Conference (APBC2022) April 26-28, 2022*
- [23] Azam, N. A., Zhu, J., Haraguchi, K., Zhao, L., Nagamochi, H., Akutsu, T.: Molecular design based on artificial neural networks, integer programming and grid neighbor search. *BIBM 2021: 360–363* (2021)
- [24] Azam, N. A., Zhu, J., Sun, Y., Shi, Y., Shurbevski, A., Zhao, L., Nagamochi, H., Akutsu, T.: A novel method for inference of acyclic chemical compounds with bounded branch-height based on artificial neural networks and integer programming. *Algorithms for Molecular Biology* 16, 18 (2021)
- [25] Tibshirani, R.: Regression shrinkage and selection via the lasso. *J. R. Statist. Soc. B* 58, 267–288 (1996)
- [26] Zhu, J., Haraguchi, K., Nagamochi, H., Akutsu, T.: Adjustive linear regression and its application to the inverse QSAR. *13th International Conference on Bioinformatics Models, Methods and Algorithms February 9-11. #14, 144–151* (2022)

- [27] Annotations from HSDB (on pubchem): |<https://pubchem.ncbi.nlm.nih.gov/>—
- [28] Jalali-Heravi, M., Fatemi, M.: Artificial neural network modeling of Kovats retention indices for noncyclic and monocyclic terpenes (2001) |[https://doi.org/10.1016/S0021-9673\(00\)01274-7](https://doi.org/10.1016/S0021-9673(00)01274-7)—
- [29] Duchowicz, P., Castro, E. A., Toropov, A. A.: Improved QSPR analysis of standard entropy of acyclic and aromatic compounds using optimized correlation weights of linear graph invariants (2002) |[https://doi.org/10.1016/S0097-8485\(01\)00121-8](https://doi.org/10.1016/S0097-8485(01)00121-8)—
- [30] Roy, K., Saha, A.: Comparative QSPR studies with molecular connectivity, molecular negentropy and TAU indices (2003) |<https://doi.org/10.1007/s00894-003-0135-z>—
- [31] Goussard, V., Duprat, F., Gerbaud, V., Ploix, J.-J., Dreyfus, G., Nardello-Rataj, V., Aubry, J.-M.: Predicting the surface tension of liquids: comparison of four modeling approaches and application to cosmetic oils. *J. Chem. Inf. Model.* 57, 12, 2986–2995 (2017) |<https://pubs.acs.org/doi/full/10.1021/acs.jClm.7b00512>—
- [32] Goussard, V., Duprat F., Ploix, J.-L., Dreyfus, G., Nardello-Rataj, V., Aubry, J.-M.: A new machine-learning tool for fast estimation of liquid viscosity. Application to cosmetic oils. *J. Chem. Inf. Model.* 60, 4, 2012–2023 (2020) |<https://pubs.acs.org/doi/10.1021/acs.jcim.0c00083>—
- [33] Naef, R.: Calculation of the isobaric heat capacities of the liquid and solid phase of organic compounds at and around 298.15 K based on their “true” molecular volume. *Molecules* 24 (8) (2019), |<https://www.mdpi.com/1420-3049/24/8/1626>—
- [34] Xiao, N.: Lipophilicity Dataset - logD7.4 of 1,130 Compounds. figshare. Dataset (2017) |<https://doi.org/10.6084/m9.figshare.5596750.v1>—
- [35] Yuan, S., Jiao, Z., Quddus, N., Kwon, J. S., Mashuga, C. V.: Developing quantitative structure–property relationship models to predict the upper flammability limit using machine learning. *Industrial & Engineering Chemistry Research* 58(8):3531-7 (2019)
- [36] Ponce, Y. M.: Total and local quadratic indices of the molecular pseudograph’s atom adjacency matrix: Applications to the prediction of physical properties of organic compounds. *Molecules* 8:687–726 (2003) |<https://www.mdpi.com/1420-3049/8/9/687>—
- [37] ESOL at MoleculeNet: |<https://moleculenet.org/datasets-1>—
- [38] Bicerano, J.: Prediction of Polymer Properties. 3rd Edition, Revised and Expanded. CRC Press (2002)
- [39] Draper, N. R., Smith, H.: Applied Regression Analysis. Wiley, New York, page 339 (1966)

Appendix

A A Full Description of Descriptors

Associated with the two functions α and β in a chemical graph $\mathbb{C} = (H, \alpha, \beta)$, we introduce functions $ac : V(E) \rightarrow (\Lambda \setminus \{\mathbf{H}\}) \times (\Lambda \setminus \{\mathbf{H}\}) \times [1, 3]$, $cs : V(E) \rightarrow (\Lambda \setminus \{\mathbf{H}\}) \times [1, 6]$ and $ec : V(E) \rightarrow ((\Lambda \setminus \{\mathbf{H}\}) \times [1, 6]) \times ((\Lambda \setminus \{\mathbf{H}\}) \times [1, 6]) \times [1, 3]$ in the following.

To represent a feature of the exterior of \mathbb{C} , a chemical rooted tree in $\mathcal{T}(\mathbb{C})$ is called a *fringe-configuration* of \mathbb{C} .

We also represent leaf-edges in the exterior of \mathbb{C} . For a leaf-edge $uv \in E(\langle\mathbb{C}\rangle)$ with $\deg_{\langle\mathbb{C}\rangle}(u) = 1$, we define the *adjacency-configuration* of e to be an ordered tuple $(\alpha(u), \alpha(v), \beta(uv))$. Define

$$\Gamma_{ac}^{\text{lf}} \triangleq \{(\mathbf{a}, \mathbf{b}, m) \mid \mathbf{a}, \mathbf{b} \in \Lambda, m \in [1, \min\{\text{val}(\mathbf{a}), \text{val}(\mathbf{b})\}]\}$$

as a set of possible adjacency-configurations for leaf-edges.

To represent a feature of an interior-vertex $v \in V^{\text{int}}(\mathbb{C})$ such that $\alpha(v) = \mathbf{a}$ and $\deg_{\langle\mathbb{C}\rangle}(v) = d$ (i.e., the number of non-hydrogen atoms adjacent to v is d) in a chemical graph $\mathbb{C} = (H, \alpha, \beta)$, we use a pair $(\mathbf{a}, d) \in (\Lambda \setminus \{\mathbf{H}\}) \times [1, 4]$, which we call the *chemical symbol* $cs(v)$ of the vertex v . We treat (\mathbf{a}, d) as a single symbol \mathbf{ad} , and define Λ_{dg} to be the set of all chemical symbols $\mu = \mathbf{ad} \in (\Lambda \setminus \{\mathbf{H}\}) \times [1, 4]$.

We define a method for featuring interior-edges as follows. Let $e = uv \in E^{\text{int}}(\mathbb{C})$ be an interior-edge $e = uv \in E^{\text{int}}(\mathbb{C})$ such that $\alpha(u) = \mathbf{a}$, $\alpha(v) = \mathbf{b}$ and $\beta(e) = m$ in a chemical graph $\mathbb{C} = (H, \alpha, \beta)$. To feature this edge e , we use a tuple $(\mathbf{a}, \mathbf{b}, m) \in (\Lambda \setminus \{\mathbf{H}\}) \times (\Lambda \setminus \{\mathbf{H}\}) \times [1, 3]$, which we call the *adjacency-configuration* $ac(e)$ of the edge e . We introduce a total order $<$ over the elements in Λ to distinguish between $(\mathbf{a}, \mathbf{b}, m)$ and $(\mathbf{b}, \mathbf{a}, m)$ ($\mathbf{a} \neq \mathbf{b}$) notationally. For a tuple $\nu = (\mathbf{a}, \mathbf{b}, m)$, let $\bar{\nu}$ denote the tuple $(\mathbf{b}, \mathbf{a}, m)$.

Let $e = uv \in E^{\text{int}}(\mathbb{C})$ be an interior-edge $e = uv \in E^{\text{int}}(\mathbb{C})$ such that $cs(u) = \mu$, $cs(v) = \mu'$ and $\beta(e) = m$ in a chemical graph $\mathbb{C} = (H, \alpha, \beta)$. To feature this edge e , we use a tuple $(\mu, \mu', m) \in \Lambda_{\text{dg}} \times \Lambda_{\text{dg}} \times [1, 3]$, which we call the *edge-configuration* $ec(e)$ of the edge e . We introduce a total order $<$ over the elements in Λ_{dg} to distinguish between (μ, μ', m) and (μ', μ, m) ($\mu \neq \mu'$) notationally. For a tuple $\gamma = (\mu, \mu', m)$, let $\bar{\gamma}$ denote the tuple (μ', μ, m) .

Let π be a chemical property for which we will construct a prediction function η from a feature vector $f(\mathbb{C})$ of a chemical graph \mathbb{C} to a predicted value $y \in \mathbb{R}$ for the chemical property of \mathbb{C} .

We first choose a set Λ of chemical elements and then collect a data set \mathcal{C}_π of chemical compounds C whose chemical elements belong to Λ , where we regard \mathcal{C}_π as a set of chemical graphs \mathbb{C} that represent the chemical compounds C in \mathcal{C}_π . To define the interior/exterior of chemical graphs $\mathbb{C} \in \mathcal{C}_\pi$, we next choose a branch-parameter ρ , where we recommend $\rho = 2$.

Let $\Lambda^{\text{int}}(\mathcal{C}_\pi) \subseteq \Lambda$ (resp., $\Lambda^{\text{ex}}(\mathcal{C}_\pi) \subseteq \Lambda$) denote the set of chemical elements used in the set $V^{\text{int}}(\mathbb{C})$ of interior-vertices (resp., the set $V^{\text{ex}}(\mathbb{C})$ of exterior-vertices) of \mathbb{C} over all chemical graphs $\mathbb{C} \in \mathcal{C}_\pi$, and $\Gamma^{\text{int}}(\mathcal{C}_\pi)$ denote the set of edge-configurations used in the set $E^{\text{int}}(\mathbb{C})$ of interior-edges in \mathbb{C} over all chemical graphs $\mathbb{C} \in \mathcal{C}_\pi$. Let $\mathcal{F}(\mathcal{C}_\pi)$ denote the set of chemical rooted trees ψ r-isomorphic to a chemical rooted tree in $\mathcal{T}(\mathbb{C})$ over all chemical graphs $\mathbb{C} \in \mathcal{C}_\pi$, where possibly a chemical rooted tree $\psi \in \mathcal{F}(\mathcal{C}_\pi)$ consists of a single chemical element $\mathbf{a} \in \Lambda \setminus \{\mathbf{H}\}$.

We define an integer encoding of a finite set A of elements to be a bijection $\sigma : A \rightarrow [1, |A|]$, where we denote by $[A]$ the set $[1, |A|]$ of integers. Introduce an integer coding of each of the sets $\Lambda^{\text{int}}(\mathcal{C}_\pi)$, $\Lambda^{\text{ex}}(\mathcal{C}_\pi)$, $\Gamma^{\text{int}}(\mathcal{C}_\pi)$ and $\mathcal{F}(\mathcal{C}_\pi)$. Let $[\mathbf{a}]^{\text{int}}$ (resp., $[\mathbf{a}]^{\text{ex}}$) denote the coded integer of an element $\mathbf{a} \in \Lambda^{\text{int}}(\mathcal{C}_\pi)$ (resp., $\mathbf{a} \in \Lambda^{\text{ex}}(\mathcal{C}_\pi)$), $[\gamma]$ denote the coded integer of an element γ in $\Gamma^{\text{int}}(\mathcal{C}_\pi)$ and $[\psi]$ denote an element ψ in $\mathcal{F}(\mathcal{C}_\pi)$.

Over 99% of chemical compounds \mathbb{C} with up to 100 non-hydrogen atoms in PubChem have degree at most 4 in the hydrogen-suppressed graph $\langle \mathbb{C} \rangle$ [24]. We assume that a chemical graph \mathbb{C} treated in this paper satisfies $\deg_{\langle \mathbb{C} \rangle}(v) \leq 4$ in the hydrogen-suppressed graph $\langle \mathbb{C} \rangle$.

In our model, we use an integer $\text{mass}^*(\mathbf{a}) = \lfloor 10 \cdot \text{mass}(\mathbf{a}) \rfloor$, for each $\mathbf{a} \in \Lambda$.

For a chemical property π , we define a set $D_\pi^{(1)}$ of descriptors of a chemical graph $\mathbb{C} = (H, \alpha, \beta) \in \mathcal{C}_\pi$ to be the following non-negative integers $\text{dcp}_i(\mathbb{C})$, $i \in [1, K_1]$, where $K_1 = 14 + |\Lambda^{\text{int}}(\mathcal{C}_\pi)| + |\Lambda^{\text{ex}}(\mathcal{C}_\pi)| + |\Gamma^{\text{int}}(\mathcal{C}_\pi)| + |\mathcal{F}(\mathcal{C}_\pi)| + |\Gamma_{\text{ac}}^{\text{lf}}|$.

1. $\text{dcp}_1(\mathbb{C})$: the number $|V(H)| - |V_{\text{H}}|$ of non-hydrogen atoms in \mathbb{C} .
2. $\text{dcp}_2(\mathbb{C})$: the rank of \mathbb{C} (i.e., the minimum number of edges to be removed to make the graph acyclic).
3. $\text{dcp}_3(\mathbb{C})$: the number $|V^{\text{int}}(\mathbb{C})|$ of interior-vertices in \mathbb{C} .
4. $\text{dcp}_4(\mathbb{C})$: the average $\overline{\text{ms}}(\mathbb{C})$ of mass^* over all atoms in \mathbb{C} ;
i.e., $\overline{\text{ms}}(\mathbb{C}) \triangleq \frac{1}{|V(H)|} \sum_{v \in V(H)} \text{mass}^*(\alpha(v))$.
5. $\text{dcp}_i(\mathbb{C})$, $i = 4 + d, d \in [1, 4]$: the number $\text{dg}_d^{\overline{\text{H}}}(\mathbb{C})$ of non-hydrogen vertices $v \in V(H) \setminus V_{\text{H}}$ of degree $\deg_{\langle \mathbb{C} \rangle}(v) = d$ in the hydrogen-suppressed chemical graph $\langle \mathbb{C} \rangle$.
6. $\text{dcp}_i(\mathbb{C})$, $i = 8 + d, d \in [1, 4]$: the number $\text{dg}_d^{\text{int}}(\mathbb{C})$ of interior-vertices of interior-degree $\deg_{\mathbb{C}^{\text{int}}}(v) = d$ in the interior $\mathbb{C}^{\text{int}} = (V^{\text{int}}(\mathbb{C}), E^{\text{int}}(\mathbb{C}))$ of \mathbb{C} .
7. $\text{dcp}_i(\mathbb{C})$, $i = 12 + m, m \in [2, 3]$: the number $\text{bd}_m^{\text{int}}(\mathbb{C})$ of interior-edges with bond multiplicity m in \mathbb{C} ; i.e., $\text{bd}_m^{\text{int}}(\mathbb{C}) \triangleq |\{e \in E^{\text{int}}(\mathbb{C}) \mid \beta(e) = m\}|$.
8. $\text{dcp}_i(\mathbb{C})$, $i = 14 + [\mathbf{a}]^{\text{int}}$, $\mathbf{a} \in \Lambda^{\text{int}}(\mathcal{C}_\pi)$: the frequency $\text{na}_{\mathbf{a}}^{\text{int}}(\mathbb{C}) = |V_{\mathbf{a}}(\mathbb{C}) \cap V^{\text{int}}(\mathbb{C})|$ of chemical element \mathbf{a} in the set $V^{\text{int}}(\mathbb{C})$ of interior-vertices in \mathbb{C} .
9. $\text{dcp}_i(\mathbb{C})$, $i = 14 + |\Lambda^{\text{int}}(\mathcal{C}_\pi)| + [\mathbf{a}]^{\text{ex}}$, $\mathbf{a} \in \Lambda^{\text{ex}}(\mathcal{C}_\pi)$: the frequency $\text{na}_{\mathbf{a}}^{\text{ex}}(\mathbb{C}) = |V_{\mathbf{a}}(\mathbb{C}) \cap V^{\text{ex}}(\mathbb{C})|$ of chemical element \mathbf{a} in the set $V^{\text{ex}}(\mathbb{C})$ of exterior-vertices in \mathbb{C} .
10. $\text{dcp}_i(\mathbb{C})$, $i = 14 + |\Lambda^{\text{int}}(\mathcal{C}_\pi)| + |\Lambda^{\text{ex}}(\mathcal{C}_\pi)| + [\gamma]$, $\gamma \in \Gamma^{\text{int}}(\mathcal{C}_\pi)$: the frequency $\text{ec}_\gamma(\mathbb{C})$ of edge-configuration γ in the set $E^{\text{int}}(\mathbb{C})$ of interior-edges in \mathbb{C} .
11. $\text{dcp}_i(\mathbb{C})$, $i = 14 + |\Lambda^{\text{int}}(\mathcal{C}_\pi)| + |\Lambda^{\text{ex}}(\mathcal{C}_\pi)| + |\Gamma^{\text{int}}(\mathcal{C}_\pi)| + [\psi]$, $\psi \in \mathcal{F}(\mathcal{C}_\pi)$: the frequency $\text{fc}_\psi(\mathbb{C})$ of fringe-configuration ψ in the set of ρ -fringe-trees in \mathbb{C} .
12. $\text{dcp}_i(\mathbb{C})$, $i = 14 + |\Lambda^{\text{int}}(\mathcal{C}_\pi)| + |\Lambda^{\text{ex}}(\mathcal{C}_\pi)| + |\Gamma^{\text{int}}(\mathcal{C}_\pi)| + |\mathcal{F}(\mathcal{C}_\pi)| + [\nu]$, $\nu \in \Gamma_{\text{ac}}^{\text{lf}}$: the frequency $\text{ac}_\nu^{\text{lf}}(\mathbb{C})$ of adjacency-configuration ν in the set of leaf-edges in $\langle \mathbb{C} \rangle$.

In the framework for polymers [22], a polymer is treated as a chemical graph of its repeating unit, where we call an edge e a *link-edge* when it lays on any path between the two joint-points of the repeating unit, and call the end-vertices of a link-edge *connecting-vertices*. The set of descriptors for a polymer is defined analogously with the above set for a monomer except for $\text{dcp}_2(\mathbb{C})$ is replaced with the number of link-edges and the following two kinds of descriptors are added: the frequency $\text{ec}_\gamma(\mathbb{C})$ of edge-configuration γ of link-edges; and the frequency of chemical symbols of connecting-vertices (see [22] for the details).

In this paper, we introduce a set of quadratic descriptors. For this, we first normalize each descriptor $\text{dcp}_i(\mathbb{C}), i \in [1, K_1]$ to a value $x(i)$ between 0 and 1 by scaling the minimum and maximum values to 0 and 1, respectively. Then construct a set $D_\pi^{(2)} := \{x(i)x(j) \mid 1 \leq i \leq j \leq K_1\} \cup \{x(i)(1-x(j)) \mid 1 \leq i, j \leq K_1\}$ of $(3(K_1)^2 + K_1)/2$ quadratic descriptors. In this paper, we reduce the union $D_\pi^{(1)} \cup D_\pi^{(2)}$ to a subset to construct a prediction function.

B Methods for Reducing Descriptors

Let \mathcal{C} be a set of components, D be a set of all descriptors and $K^* \in [1, |D|]$ be a number of descriptors we want to choose from D .

Given a data set \mathcal{C} , a set D of descriptors and a real $\lambda > 0$, let $\text{Des-set-LLR}(\mathcal{C}, D, \lambda)$ denote the set S of descriptors $d \in D$ such that $w(d) = 0$ for the hyperplane (w, b) output by $\text{LLR}(\mathcal{C}, D, \lambda)$ (where we numerically treat $w(d)$ with $|w(d)| \leq 10^{-6}$ as 0 in our experiment).

B.1 A method based on Lasso linear regression

Since the Lasso linear regression finds some number of descriptors $d \in D$ with $w(d) = 0$ in the output hyperplane (w, b) , we can reduce a given set of descriptors by applying the Lasso linear regression repeatedly. Choose parameters c_{\max} and d_{\max} so that $\text{LLR}(\mathcal{C}, D, \lambda)$ can be executed in a reasonable running time when $|\mathcal{C}| \leq c_{\max}$ and $|D| \leq d_{\max}$. Let $\tilde{K} \in [1, |D|]$ be an integer for the number of descriptors that we choose from a given set D of descriptors.

$\text{LLR-Reduce}(\mathcal{C}, D)$:

Input: A data set \mathcal{C} and a set D of descriptors;

Output: A subset $\tilde{D} \subseteq D$ with $|\tilde{D}| = \tilde{K}$.

Initialize $D' := D$;

while $|D'| > \tilde{K}$ **do**

Partition D' randomly into disjoint subsets D_1, D_2, \dots, D_p such that $|D_i| \leq d_{\max}$ for each i ;

for each $i = 1, 2, \dots, p$ **do**

Choose a subset \mathcal{C}_i with $|\mathcal{C}_i| = \min\{c_{\max}, |\mathcal{C}|\}$ of \mathcal{C} randomly;

$D'_i := \text{Des-set-LLR}(\mathcal{C}_i, D_i, \lambda)$ for some $\lambda > 0$

endfor;

$D' := D'_1 \cup D'_2 \cup \dots \cup D'_p$

endwhile;

Output $\tilde{D} := D'$ after adding to D' extra $\tilde{K} - |D'|$ descriptors from the previous set D' when

$|D'| < \tilde{K}$ by using the K-best method.

In this paper, we set $c_{\max} := 200$, $d_{\max} := 200$ and $\tilde{K} := 5000$ in our computational experiment.

B.2 A method based on backward stepwise procedure

A backward stepwise procedure [39] reduces the number of descriptors one by one choosing the one removal of which maximizes the learning performance and outputs a subset with the maximum learning performance among all subsets during the reduction iteration.

For a subset $S \subseteq D$ and a positive integer p , let $R_{\text{CV,MLR}}^2(\mathcal{C}, S, p)$ denote $R_{\text{CV}}^2(\mathcal{C}, S, p)$ for constructing a prediction function $\eta_{w,b}$ by $\text{MLR}(\mathcal{C}, S)$. We define a performance evaluation function $g_p : 2^D \rightarrow \mathbb{R}$ for an integer $p \geq 1$ such that $g_p(S) = R_{\text{CV,MLR}}^2(\mathcal{C}, S, p)$. The backward stepwise procedure with this function g_p is described as follows.

BS-Reduce(\mathcal{C}, D, p):

Input: A data set \mathcal{C} , a set D of descriptors, an integer $p \geq 1$ and a performance evaluation function $g_p : 2^D \rightarrow \mathbb{R}$ defined above;

Output: A subset $D^* \subseteq D$.

Compute $\ell_{\text{best}} := g_p(D)$; Initialize $D_{\text{best}} := D' := D$;

while $D' \neq \emptyset$ **do**

 Compute $\ell(d) := g_p(D' \setminus \{d\})$ for each descriptor $d \in D'$;

 Set $d^* \in D'$ to be a descriptor that maximizes $\ell(d)$ over all $d \in D'$;

 Update: $D' := D' \setminus \{d^*\}$;

if $\ell(d^*) > \ell_{\text{best}}$ **then** update $D_{\text{best}} := D'$ and $\ell_{\text{best}} := \ell(d^*)$ **endif**

endwhile;

Output $D^* := D_{\text{best}}$.

Based on the Lasso linear regression and the backward stepwise procedure, we design the following method for choosing a subset D^* of a given set D of descriptors. We are given a give set A of 17 real numbers and a set $B(a)$ of 16 real numbers close to each number $a \in A$. The method first choose a best parameter $\lambda_{\text{best}} \in A$ to construct a prediction function by LLR and then choose a subset $D_i \subseteq D$ for each $\lambda_i \in B(\lambda_{\text{best}})$ by the backward stepwise procedure. The procedure takes $O(|D|^2)$ iterations which may take a large amount of running time. We introduce an upper bound s_{\max} on the size of an input descriptor D for the backward stepwise procedure. Let p_1 , p_2 and p_3 be integer parameters that control the number of executions of cross-validations to evaluate the learning performance in the method.

Select-Des-set(\mathcal{C}, D):

Input: A data set \mathcal{C} , a set D of descriptors,

a set $A = \{0, 10^{-6}, 10^{-5}, 10^{-4}, 10^{-3}, 0.01, 0.05, 0.1, 0.5, 0.75, 1, 2, 5, 10, 25, 50, 100\}$, and

a set $B(\lambda)$ of 16 real numbers close to each $\lambda \in A$;

Output: A subset D^* of D .

for each $\lambda \in A$ **do**

 Compute $D_\lambda := \text{Des-set-LLR}(\mathcal{C}, D, \lambda)$ and $\ell_\lambda := R_{\text{CV,MLR}}^2(\mathcal{C}, D_\lambda, p_1)$

endfor;

Set λ_{best} to be a $\lambda \in A$ that maximizes ℓ_λ ; Denote $B(\lambda_{\text{best}})$ by $\{\lambda_1, \lambda_2, \dots, \lambda_{16}\}$;

for each $i \in [1, 16]$ **do**

Compute $D_i := \text{Des-set-LLR}(\mathcal{C}, D, \lambda_i)$ and let $(w, b), w \in \mathbb{R}^{|D|}, b \in \mathbb{R}$ be the hyperplane obtained by this LLR;

if $|D_i| \leq s_{\text{max}}$ **then**

$D'_i := D_i$

else

Let D'_i consist of s_{max} descriptors $d \in D_i$ that have the s_{max} largest absolute values $|w(d)|$ in the weight sets $\{w(d) \mid d \in D_i\}$ of the hyperplane (w, b)

endif;

$D_i^\dagger := \text{BS-Reduce}(\mathcal{C}, D'_i, p_2)$; $\ell_i := \text{R}_{\text{CV,MLR}}^2(\mathcal{C}, D_i^\dagger, p_3)$

endfor;

Set D^* to be a set D_i^\dagger that maximizes $\ell_i, i \in [1, 16]$.

In our computational experiment in this paper, we set $p_1 := p_2 := p_3 := 5$ and $s_{\text{max}} := 150 + 10^4 / (|\mathcal{C}| + 200)$.

C Specifying Target Chemical Graphs

Given a prediction function η and a target value $y^* \in \mathbb{R}$, we call a chemical graph \mathbb{C}^* such that $\eta(x^*) = y^*$ for the feature vector $x^* = f(\mathbb{C}^*)$ a *target chemical graph*. This section presents a set of rules for specifying topological substructure of a target chemical graph in a flexible way in Stage 4.

We first describe how to reduce a chemical graph $\mathbb{C} = (H, \alpha, \beta)$ into an abstract form based on which our specification rules will be defined. To illustrate the reduction process, we use the chemical graph $\mathbb{C} = (H, \alpha, \beta)$ such that $\langle \mathbb{C} \rangle$ is given in Figure 2.

R1 Removal of all ρ -fringe-trees: The interior $H^{\text{int}} = (V^{\text{int}}(\mathbb{C}), E^{\text{int}}(\mathbb{C}))$ of \mathbb{C} is obtained by removing the non-root vertices of each ρ -fringe-trees $\mathbb{C}[u] \in \mathcal{T}(\mathbb{C}), u \in V^{\text{int}}(\mathbb{C})$. Figure 8 illustrates the interior H^{int} of chemical graph \mathbb{C} with $\rho = 2$ in Figure 2.

R2 Removal of some leaf paths: We call a u, v -path Q in H^{int} a *leaf path* if vertex v is a leaf-vertex of H^{int} and the degree of each internal vertex of Q in H^{int} is 2, where we regard that Q is rooted at vertex u . A connected subgraph S of the interior H^{int} of \mathbb{C} is called a *cyclical-base* if S is obtained from H by removing the vertices in $V(Q_u) \setminus \{u\}, u \in X$ for a subset X of interior-vertices and a set $\{Q_u \mid u \in X\}$ of leaf u, v -paths Q_u such that no two paths Q_u and $Q_{u'}$ share a vertex. Figure 9(a) illustrates a cyclical-base $S = H^{\text{int}} - \bigcup_{u \in X} (V(Q_u) \setminus \{u\})$ of the interior H^{int} for a set $\{Q_{u_5} = (u_5, u_{24}), Q_{u_{18}} = (u_{18}, u_{25}, u_{26}, u_{27}), Q_{u_{22}} = (u_{22}, u_{28})\}$ of leaf paths in Figure 8.

R3 Contraction of some pure paths: A path in S is called *pure* if each internal vertex of the path is of degree 2. Choose a set \mathcal{P} of several pure paths in S so that no two paths share vertices except for their end-vertices. A graph S' is called a *contraction* of a graph S (with respect to \mathcal{P}) if S' is obtained from S by replacing each pure u, v -path with a

single edge $a = uv$, where S' may contain multiple edges between the same pair of adjacent vertices. Figure 9(b) illustrates a contraction S' obtained from the chemical graph S by contracting each uv -path $P_a \in \mathcal{P}$ into a new edge $a = uv$, where $a_1 = u_1u_2$, $a_2 = u_1u_3$, $a_3 = u_4u_7$, $a_4 = u_{10}u_{11}$ and $a_5 = u_{11}u_{12}$ and $\mathcal{P} = \{P_{a_1} = (u_1, u_{13}, u_2), P_{a_2} = (u_1, u_{14}, u_3), P_{a_3} = (u_4, u_{15}, u_{16}, u_7), P_{a_4} = (u_{10}, u_{17}, u_{18}, u_{19}, u_{11}), P_{a_5} = (u_{11}, u_{20}, u_{21}, u_{22}, u_{12})\}$ of pure paths in Figure 9(a).

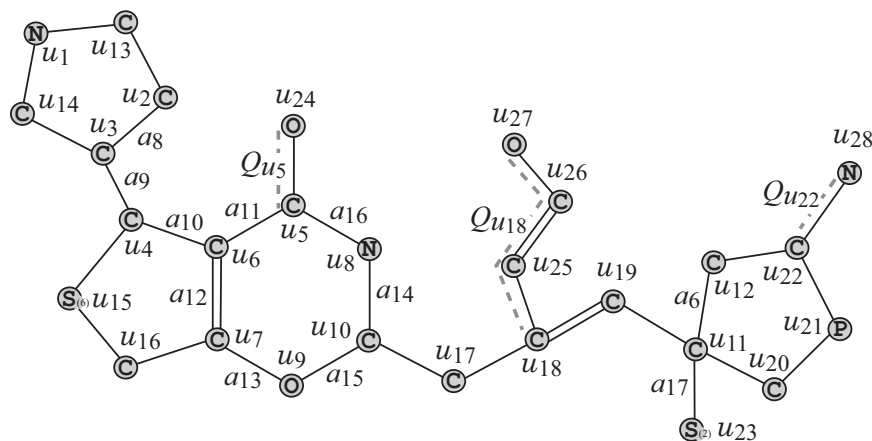


Figure 8: The interior H^{int} of chemical graph \mathbb{C} with $\langle \mathbb{C} \rangle$ in Figure 2 for $\rho = 2$.

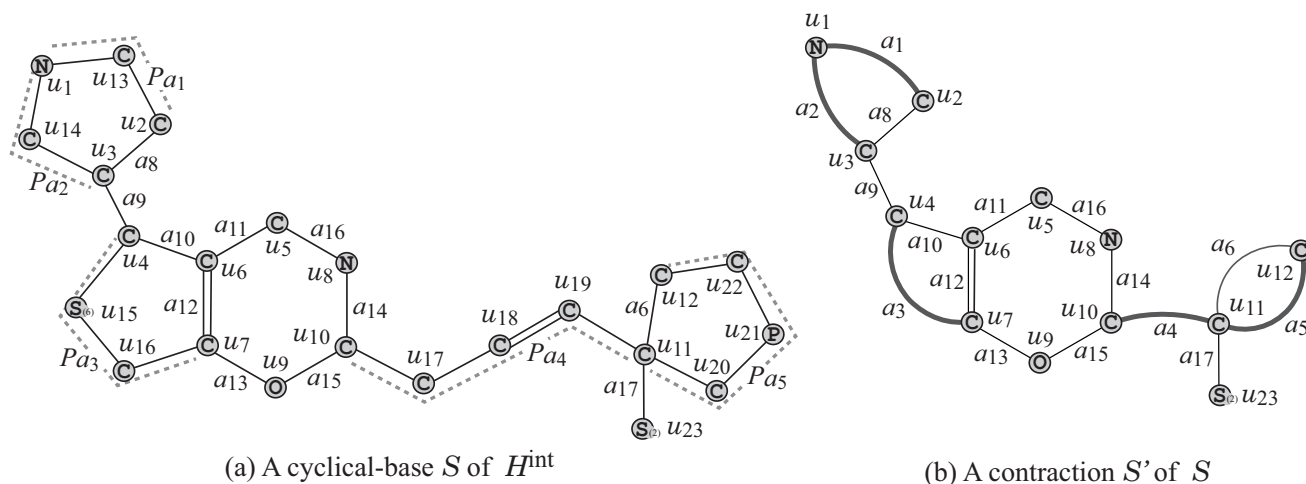


Figure 9: (a) A cyclical-base $S = H^{\text{int}} - \bigcup_{u \in \{u_5, u_{18}, u_{22}\}} (V(Q_u) \setminus \{u\})$ of the interior H^{int} in Figure 8; (b) A contraction S' of S for a pure path set $\mathcal{P} = \{P_{a_1}, P_{a_2}, \dots, P_{a_5}\}$ in (a), where a new edge obtained by contracting a pure path is depicted with a thick line.

We will define a set of rules so that a chemical graph can be obtained from a graph (called a seed graph in the next section) by applying processes R3 to R1 in a reverse way. We specify topological substructures of a target chemical graph with a tuple $(G_C, \sigma_{\text{int}}, \sigma_{\text{ce}})$ called a *target specification* defined under the set of the following rules.

Seed Graph

A *seed graph* $G_C = (V_C, E_C)$ is defined to be a graph (possibly with multiple edges) such that the edge set E_C consists of four sets $E_{(\geq 2)}$, $E_{(\geq 1)}$, $E_{(0/1)}$ and $E_{(=1)}$, where each of them can be empty. A seed graph plays a role of the most abstract form S' in R3. Figure 4(a) illustrates an example of a seed graph G_C with $r(G_C) = 5$, where $V_C = \{u_1, u_2, \dots, u_{12}, u_{23}\}$, $E_{(\geq 2)} = \{a_1, a_2, \dots, a_5\}$, $E_{(\geq 1)} = \{a_6\}$, $E_{(0/1)} = \{a_7\}$ and $E_{(=1)} = \{a_8, a_9, \dots, a_{16}\}$.

A *subdivision* S of G_C is a graph constructed from a seed graph G_C according to the following rules:

- Each edge $e = uv \in E_{(\geq 2)}$ is replaced with a u, v -path P_e of length at least 2;
- Each edge $e = uv \in E_{(\geq 1)}$ is replaced with a u, v -path P_e of length at least 1 (equivalently e is directly used or replaced with a u, v -path P_e of length at least 2);
- Each edge $e \in E_{(0/1)}$ is either used or discarded, where $E_{(0/1)}$ is required to be chosen as a non-separating edge subset of $E(G_C)$ since otherwise the connectivity of a final chemical graph \mathbb{C} is not guaranteed; $r(\mathbb{C}) = r(G_C) - |E'|$ holds for a subset $E' \subseteq E_{(0/1)}$ of edges discarded in a final chemical graph \mathbb{C} ; and
- Each edge $e \in E_{(=1)}$ is always used directly.

We allow a possible elimination of edges in $E_{(0/1)}$ as an optional rule in constructing a target chemical graph from a seed graph, even though such an operation has not been included in the process R3. A subdivision S plays a role of a cyclical-base in R2. A target chemical graph $\mathbb{C} = (H, \alpha, \beta)$ will contain S as a subgraph of the interior H^{int} of \mathbb{C} .

Interior-specification

A graph H^* that serves as the interior H^{int} of a target chemical graph \mathbb{C} will be constructed as follows. First construct a subdivision S of a seed graph G_C by replacing each edge $e = uu' \in E_{(\geq 2)} \cup E_{(\geq 1)}$ with a pure u, u' -path P_e . Next construct a supergraph H^* of S by attaching a leaf path Q_v at each vertex $v \in V_C$ or at an internal vertex $v \in V(P_e) \setminus \{u, u'\}$ of each pure u, u' -path P_e for some edge $e = uu' \in E_{(\geq 2)} \cup E_{(\geq 1)}$, where possibly $Q_v = (v)$, $E(Q_v) = \emptyset$ (i.e., we do not attach any new edges to v). We introduce the following rules for specifying the size of H^* , the length $|E(P_e)|$ of a pure path P_e , the length $|E(Q_v)|$ of a leaf path Q_v , the number of leaf paths Q_v and a bond-multiplicity of each interior-edge, where we call the set of prescribed constants an *interior-specification* σ_{int} :

- Lower and upper bounds $n_{\text{LB}}^{\text{int}}, n_{\text{UB}}^{\text{int}} \in \mathbb{Z}_+$ on the number of interior-vertices of a target chemical graph \mathbb{C} .
- For each edge $e = uu' \in E_{(\geq 2)} \cup E_{(\geq 1)}$,
 - a lower bound $\ell_{\text{LB}}(e)$ and an upper bound $\ell_{\text{UB}}(e)$ on the length $|E(P_e)|$ of a pure u, u' -path P_e . (For a notational convenience, set $\ell_{\text{LB}}(e) := 0$, $\ell_{\text{UB}}(e) := 1$, $e \in E_{(0/1)}$ and $\ell_{\text{LB}}(e) := 1$, $\ell_{\text{UB}}(e) := 1$, $e \in E_{(=1)}$.)

a lower bound $\text{bl}_{\text{LB}}(e)$ and an upper bound $\text{bl}_{\text{UB}}(e)$ on the number of leaf paths Q_v attached at internal vertices v of a pure u, u' -path P_e .

a lower bound $\text{ch}_{\text{LB}}(e)$ and an upper bound $\text{ch}_{\text{UB}}(e)$ on the maximum length $|E(Q_v)|$ of a leaf path Q_v attached at an internal vertex $v \in V(P_e) \setminus \{u, u'\}$ of a pure u, u' -path P_e .

- For each vertex $v \in V_C$,

a lower bound $\text{ch}_{\text{LB}}(v)$ and an upper bound $\text{ch}_{\text{UB}}(v)$ on the number of leaf paths Q_v attached to v , where $0 \leq \text{ch}_{\text{LB}}(v) \leq \text{ch}_{\text{UB}}(v) \leq 1$.

a lower bound $\text{ch}_{\text{LB}}(v)$ and an upper bound $\text{ch}_{\text{UB}}(v)$ on the length $|E(Q_v)|$ of a leaf path Q_v attached to v .

- For each edge $e = uu' \in E_C$, a lower bound $\text{bd}_{m,\text{LB}}(e)$ and an upper bound $\text{bd}_{m,\text{UB}}(e)$ on the number of edges with bond-multiplicity $m \in [2, 3]$ in u, u' -path P_e , where we regard $P_e, e \in E_{(0/1)} \cup E_{(=1)}$ as single edge e .

We call a graph H^* that satisfies an interior-specification σ_{int} a σ_{int} -extension of G_C , where the bond-multiplicity of each edge has been determined.

Table 8 shows an example of an interior-specification σ_{int} to the seed graph G_C in Figure 4.

Table 8: Example 1 of an interior-specification σ_{int} .

$n_{\text{LB}}^{\text{int}} = 20$	$n_{\text{UB}}^{\text{int}} = 28$					
	a_1	a_2	a_3	a_4	a_5	a_6
$\ell_{\text{LB}}(a_i)$	2	2	2	3	2	1
$\ell_{\text{UB}}(a_i)$	3	4	3	5	4	4
$\text{bl}_{\text{LB}}(a_i)$	0	0	0	1	1	0
$\text{bl}_{\text{UB}}(a_i)$	1	1	0	2	1	0
$\text{ch}_{\text{LB}}(a_i)$	0	1	0	4	3	0
$\text{ch}_{\text{UB}}(a_i)$	3	3	1	6	5	2

	u_1	u_2	u_3	u_4	u_5	u_6	u_7	u_8	u_9	u_{10}	u_{11}	u_{12}	u_{23}
$\text{bl}_{\text{LB}}(u_i)$	0	0	0	0	0	0	0	0	0	0	0	0	0
$\text{bl}_{\text{UB}}(u_i)$	1	1	1	1	1	0	0	0	0	0	0	0	0
$\text{ch}_{\text{LB}}(u_i)$	0	0	0	0	1	0	0	0	0	0	0	0	0
$\text{ch}_{\text{UB}}(u_i)$	1	0	0	0	3	0	1	1	0	1	2	4	1

	a_1	a_2	a_3	a_4	a_5	a_6	a_7	a_8	a_9	a_{10}	a_{11}	a_{12}	a_{13}	a_{14}	a_{15}	a_{16}	a_{17}
$\text{bd}_{2,\text{LB}}(a_i)$	0	0	0	1	0	0	0	0	0	0	0	1	0	0	0	0	0
$\text{bd}_{2,\text{UB}}(a_i)$	1	1	0	2	2	0	0	0	0	0	0	1	0	0	0	0	0
$\text{bd}_{3,\text{LB}}(a_i)$	0	0	0	0	0	0	0	0	0	0	0	0	0	0	0	0	0
$\text{bd}_{3,\text{UB}}(a_i)$	0	0	0	0	1	0	0	0	0	0	0	0	0	0	0	0	0

Figure 10 illustrates an example of an σ_{int} -extension H^* of seed graph G_C in Figure 4 under the interior-specification σ_{int} in Table 8.

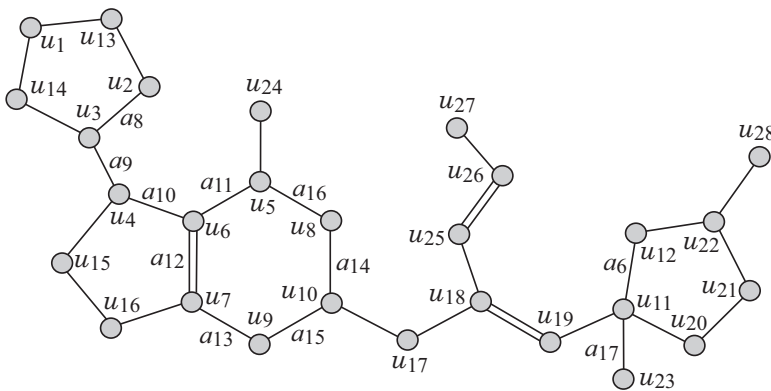


Figure 10: An illustration of a graph H^* that is obtained from the seed graph G_C in Figure 4 under the interior-specification σ_{int} in Table 8.

Chemical-specification

Let H^* be a graph that serves as the interior H^{int} of a target chemical graph \mathbb{C} , where the bond-multiplicity of each edge in H^* has been determined. Finally we introduce a set of rules for constructing a target chemical graph \mathbb{C} from H^* by choosing a chemical element $\mathbf{a} \in \Lambda$ and assigning a ρ -fringe-tree ψ to each interior-vertex $v \in V^{\text{int}}$. We introduce the following rules for specifying the size of \mathbb{C} , a set of chemical rooted trees that are allowed to use as ρ -fringe-trees and lower and upper bounds on the frequency of a chemical element, a chemical symbol, and an edge-configuration, where we call the set of prescribed constants a *chemical specification* σ_{ce} :

- Lower and upper bounds $n_{\text{LB}}, n^* \in \mathbb{Z}_+$ on the number of vertices, where $n_{\text{LB}}^{\text{int}} \leq n_{\text{LB}} \leq n^*$.
- Subsets $\mathcal{F}(v) \subseteq \mathcal{F}(D_\pi), v \in V_C$ and $\mathcal{F}_E \subseteq \mathcal{F}(D_\pi)$ of chemical rooted trees ψ with $\text{ht}(\psi) \leq \rho$, where we require that every ρ -fringe-tree $\mathbb{C}[v]$ rooted at a vertex $v \in V_C$ (resp., at an internal vertex v not in V_C) in \mathbb{C} belongs to $\mathcal{F}(v)$ (resp., \mathcal{F}_E). Let $\mathcal{F}^* := \mathcal{F}_E \cup \bigcup_{v \in V_C} \mathcal{F}(v)$ and Λ^{ex} denote the set of chemical elements assigned to non-root vertices over all chemical rooted trees in \mathcal{F}^* .
- A subset $\Lambda^{\text{int}} \subseteq \Lambda^{\text{int}}(D_\pi)$, where we require that every chemical element $\alpha(v)$ assigned to an interior-vertex v in \mathbb{C} belongs to Λ^{int} . Let $\Lambda := \Lambda^{\text{int}} \cup \Lambda^{\text{ex}}$ and $\text{na}_{\mathbf{a}}(\mathbb{C})$ (resp., $\text{na}_{\mathbf{a}}^{\text{int}}(\mathbb{C})$ and $\text{na}_{\mathbf{a}}^{\text{ex}}(\mathbb{C})$) denote the number of vertices (resp., interior-vertices and exterior-vertices) v such that $\alpha(v) = \mathbf{a}$ in \mathbb{C} .
- A set $\Lambda_{\text{dg}}^{\text{int}} \subseteq \Lambda \times [1, 4]$ of chemical symbols and a set $\Gamma^{\text{int}} \subseteq \Gamma^{\text{int}}(D_\pi)$ of edge-configurations (μ, μ', m) with $\mu \leq \mu'$, where we require that the edge-configuration $\text{ec}(e)$ of an interior-edge e in \mathbb{C} belongs to Γ^{int} . We do not distinguish (μ, μ', m) and (μ', μ, m) .
- Define $\Gamma_{\text{ac}}^{\text{int}}$ to be the set of adjacency-configurations such that $\Gamma_{\text{ac}}^{\text{int}} := \{(\mathbf{a}, \mathbf{b}, m) \mid (ad, bd', m) \in \Gamma^{\text{int}}\}$. Let $\text{ac}_\nu^{\text{int}}(\mathbb{C}), \nu \in \Gamma_{\text{ac}}^{\text{int}}$ denote the number of interior-edges e such that $\text{ac}(e) = \nu$ in \mathbb{C} .
- Subsets $\Lambda^*(v) \subseteq \{\mathbf{a} \in \Lambda^{\text{int}} \mid \text{val}(\mathbf{a}) \geq 2\}, v \in V_C$, we require that every chemical element $\alpha(v)$ assigned to a vertex $v \in V_C$ in the seed graph belongs to $\Lambda^*(v)$.

- Lower and upper bound functions $\text{na}_{\text{LB}}, \text{na}_{\text{UB}} : \Lambda \rightarrow [1, n^*]$ and $\text{na}_{\text{LB}}^{\text{int}}, \text{na}_{\text{UB}}^{\text{int}} : \Lambda^{\text{int}} \rightarrow [1, n^*]$ on the number of interior-vertices v such that $\alpha(v) = \mathbf{a}$ in \mathbb{C} .
- Lower and upper bound functions $\text{ns}_{\text{LB}}^{\text{int}}, \text{ns}_{\text{UB}}^{\text{int}} : \Lambda_{\text{dg}}^{\text{int}} \rightarrow [1, n^*]$ on the number of interior-vertices v such that $\text{cs}(v) = \mu$ in \mathbb{C} .
- Lower and upper bound functions $\text{ac}_{\text{LB}}^{\text{int}}, \text{ac}_{\text{UB}}^{\text{int}} : \Gamma_{\text{ac}}^{\text{int}} \rightarrow \mathbb{Z}_+$ on the number of interior-edges e such that $\text{ac}(e) = \nu$ in \mathbb{C} .
- Lower and upper bound functions $\text{ec}_{\text{LB}}^{\text{int}}, \text{ec}_{\text{UB}}^{\text{int}} : \Gamma^{\text{int}} \rightarrow \mathbb{Z}_+$ on the number of interior-edges e such that $\text{ec}(e) = \gamma$ in \mathbb{C} .
- Lower and upper bound functions $\text{fc}_{\text{LB}}, \text{fc}_{\text{UB}} : \mathcal{F}^* \rightarrow [0, n^*]$ on the number of interior-vertices v such that $\mathbb{C}[v]$ is r -isomorphic to $\psi \in \mathcal{F}^*$ in \mathbb{C} .
- Lower and upper bound functions $\text{ac}_{\text{LB}}^{\text{lf}}, \text{ac}_{\text{UB}}^{\text{lf}} : \Gamma_{\text{ac}}^{\text{lf}} \rightarrow [0, n^*]$ on the number of leaf-edges uv in $\text{ac}_{\mathbb{C}}$ with adjacency-configuration ν .

We call a chemical graph \mathbb{C} that satisfies a chemical specification σ_{ce} a $(\sigma_{\text{int}}, \sigma_{\text{ce}})$ -*extension of* $G_{\mathbb{C}}$, and denote by $\mathcal{G}(G_{\mathbb{C}}, \sigma_{\text{int}}, \sigma_{\text{ce}})$ the set of all $(\sigma_{\text{int}}, \sigma_{\text{ce}})$ -extensions of $G_{\mathbb{C}}$.

Table 9 shows an example of a chemical-specification σ_{ce} to the seed graph $G_{\mathbb{C}}$ in Figure 4.

Figure 2 illustrates an example \mathbb{C} of a $(\sigma_{\text{int}}, \sigma_{\text{ce}})$ -extension of $G_{\mathbb{C}}$ obtained from the σ_{int} -extension H^* in Figure 10 under the chemical-specification σ_{ce} in Table 9. Note that $r(\mathbb{C}) = r(H^*) = r(G_{\mathbb{C}}) - 1 = 4$ holds since the edge in $E_{(0/1)}$ is discarded in H^* .

D Test Instances for Inferring Chemical Graphs

We prepared the following instances (a)-(d) for conducting experiments of the second phase of the framework.

In the second phase of inferring chemical graphs, we use two properties $\pi \in \{\text{BP}, \text{DC}\}$ and define a set $\Lambda(\pi)$ of chemical elements as follows: $\Lambda(\text{BP}) = \Lambda(\text{DC}) = \Lambda_7 = \{\text{H}, \text{C}, \text{O}, \text{N}, \text{S}_{(2)}, \text{S}_{(6)}, \text{Cl}\}$.

- (a) $I_{\text{a}} = (G_{\mathbb{C}}, \sigma_{\text{int}}, \sigma_{\text{ce}})$: The instance introduced in Section C to explain the target specification. For each property π , we replace $\Lambda = \{\text{H}, \text{C}, \text{O}, \text{N}, \text{S}_{(2)}, \text{S}_{(6)}, \text{P}_{(5)}\}$ in Table 9 with $\Lambda(\pi) \cap \{\text{H}, \text{C}, \text{O}, \text{N}, \text{S}_{(2)}, \text{S}_{(6)}, \text{P}_{(5)}\} = \{\text{H}, \text{C}, \text{O}, \text{N}, \text{S}_{(2)}, \text{S}_{(6)}\}$ and remove from the σ_{ce} all chemical symbols, edge-configurations and fringe-configurations that cannot be constructed from the replaced element set (i.e., those containing a chemical element $\text{P}_{(5)}$).
- (b) $I_{\text{b}}^i = (G_{\mathbb{C}}^i, \sigma_{\text{int}}^i, \sigma_{\text{ce}}^i)$, $i = 1, 2, 3, 4$: An instance for inferring chemical graphs with rank at most 2. In the four instances I_{b}^i , $i = 1, 2, 3, 4$, the following specifications in $(\sigma_{\text{int}}, \sigma_{\text{ce}})$ are common.

Set $\Lambda := \Lambda(\pi)$ for a given property $\pi \in \{\text{BP}, \text{DC}\}$, set $\Lambda_{\text{dg}}^{\text{int}}$ to be the set of all possible symbols in $\Lambda \times [1, 4]$ that appear in the data set \mathcal{C}_{π} and set Γ^{int} to be the set of all edge-configurations that appear in the data set \mathcal{C}_{π} . Set $\Lambda^*(v) := \Lambda$, $v \in V_{\mathbb{C}}$.

Table 9: Example 2 of a chemical-specification σ_{ce} .

$n_{LB} = 30, n^* = 50.$																																																										
branch-parameter: $\rho = 2$																																																										
Each of sets $\mathcal{F}(v), v \in V_C$ and \mathcal{F}_E is set to be the set \mathcal{F} of chemical rooted trees ψ with $\text{ht}(\langle\psi\rangle) \leq \rho = 2$ in Figure 4(b).																																																										
$\Lambda = \{\text{H, C, N, O, S}_{(2)}, \text{S}_{(6)}, \text{P} = \text{P}_{(5)}\} \quad \Lambda_{\text{dg}}^{\text{int}} = \{\text{C2, C3, C4, N2, N3, O2, S}_{(2)}\text{2, S}_{(6)}\text{3, P4}\}$																																																										
$\Gamma_{\text{ac}}^{\text{int}}$	$\nu_1 = (\text{C, C, 1}), \nu_2 = (\text{C, C, 2}), \nu_3 = (\text{C, N, 1}), \nu_4 = (\text{C, O, 1}), \nu_5 = (\text{C, S}_{(2)}, 1), \nu_6 = (\text{C, S}_{(6)}, 1), \nu_7 = (\text{C, P, 1})$																																																									
Γ^{int}	$\gamma_1 = (\text{C2, C2, 1}), \gamma_2 = (\text{C2, C3, 1}), \gamma_3 = (\text{C2, C3, 2}), \gamma_4 = (\text{C2, C4, 1}), \gamma_5 = (\text{C3, C3, 1}), \gamma_6 = (\text{C3, C3, 2}),$ $\gamma_7 = (\text{C3, C4, 1}), \gamma_8 = (\text{C2, N2, 1}), \gamma_9 = (\text{C3, N2, 1}), \gamma_{10} = (\text{C3, O2, 1}), \gamma_{11} = (\text{C2, C2, 2}), \gamma_{12} = (\text{C2, O2, 1}),$ $\gamma_{13} = (\text{C3, N3, 1}), \gamma_{14} = (\text{C4, S}_{(2)}\text{2, 2}), \gamma_{15} = (\text{C2, S}_{(6)}\text{3, 1}), \gamma_{16} = (\text{C3, S}_{(6)}\text{3, 1}), \gamma_{17} = (\text{C2, P4, 2}),$ $\gamma_{18} = (\text{C3, P4, 1})$																																																									
$\Lambda^*(u_1) = \Lambda^*(u_8) = \{\text{C, N}\}, \Lambda^*(u_9) = \{\text{C, O}\}, \Lambda^*(u) = \{\text{C}\}, u \in V_C \setminus \{u_1, u_8, u_9\}$																																																										
	<table border="1"> <thead> <tr> <th></th> <th>H</th> <th>C</th> <th>N</th> <th>O</th> <th>S₍₂₎</th> <th>S₍₆₎</th> <th>P</th> </tr> </thead> <tbody> <tr> <td>na_{LB}(a)</td> <td>40</td> <td>27</td> <td>1</td> <td>1</td> <td>0</td> <td>0</td> <td>0</td> </tr> <tr> <td>na_{UB}(a)</td> <td>65</td> <td>37</td> <td>4</td> <td>8</td> <td>1</td> <td>1</td> <td>1</td> </tr> </tbody> </table> <table border="1"> <thead> <tr> <th></th> <th>C</th> <th>N</th> <th>O</th> <th>S₍₂₎</th> <th>S₍₆₎</th> <th>P</th> </tr> </thead> <tbody> <tr> <td>na_{LB}^{int}(a)</td> <td>9</td> <td>1</td> <td>0</td> <td>0</td> <td>0</td> <td>0</td> </tr> <tr> <td>na_{UB}^{int}(a)</td> <td>23</td> <td>4</td> <td>5</td> <td>1</td> <td>1</td> <td>1</td> </tr> </tbody> </table>		H	C	N	O	S ₍₂₎	S ₍₆₎	P	na _{LB} (a)	40	27	1	1	0	0	0	na _{UB} (a)	65	37	4	8	1	1	1		C	N	O	S ₍₂₎	S ₍₆₎	P	na _{LB} ^{int} (a)	9	1	0	0	0	0	na _{UB} ^{int} (a)	23	4	5	1	1	1												
	H	C	N	O	S ₍₂₎	S ₍₆₎	P																																																			
na _{LB} (a)	40	27	1	1	0	0	0																																																			
na _{UB} (a)	65	37	4	8	1	1	1																																																			
	C	N	O	S ₍₂₎	S ₍₆₎	P																																																				
na _{LB} ^{int} (a)	9	1	0	0	0	0																																																				
na _{UB} ^{int} (a)	23	4	5	1	1	1																																																				
	<table border="1"> <thead> <tr> <th></th> <th>C2</th> <th>C3</th> <th>C4</th> <th>N2</th> <th>N3</th> <th>O2</th> <th>S₍₂₎2</th> <th>S₍₆₎3</th> <th>P4</th> </tr> </thead> <tbody> <tr> <td>ns_{LB}^{int}(μ)</td> <td>3</td> <td>5</td> <td>0</td> <td>0</td> <td>0</td> <td>0</td> <td>0</td> <td>0</td> <td>0</td> </tr> <tr> <td>ns_{UB}^{int}(μ)</td> <td>8</td> <td>15</td> <td>2</td> <td>2</td> <td>3</td> <td>5</td> <td>1</td> <td>1</td> <td>1</td> </tr> </tbody> </table>		C2	C3	C4	N2	N3	O2	S ₍₂₎ 2	S ₍₆₎ 3	P4	ns _{LB} ^{int} (μ)	3	5	0	0	0	0	0	0	0	ns _{UB} ^{int} (μ)	8	15	2	2	3	5	1	1	1																											
	C2	C3	C4	N2	N3	O2	S ₍₂₎ 2	S ₍₆₎ 3	P4																																																	
ns _{LB} ^{int} (μ)	3	5	0	0	0	0	0	0	0																																																	
ns _{UB} ^{int} (μ)	8	15	2	2	3	5	1	1	1																																																	
	<table border="1"> <thead> <tr> <th></th> <th>ν_1</th> <th>ν_2</th> <th>ν_3</th> <th>ν_4</th> <th>ν_5</th> <th>ν_6</th> <th>ν_7</th> </tr> </thead> <tbody> <tr> <td>ac_{LB}^{int}(ν)</td> <td>0</td> <td>0</td> <td>0</td> <td>0</td> <td>0</td> <td>0</td> <td>0</td> </tr> <tr> <td>ac_{UB}^{int}(ν)</td> <td>30</td> <td>10</td> <td>10</td> <td>10</td> <td>1</td> <td>1</td> <td>1</td> </tr> </tbody> </table>		ν_1	ν_2	ν_3	ν_4	ν_5	ν_6	ν_7	ac _{LB} ^{int} (ν)	0	0	0	0	0	0	0	ac _{UB} ^{int} (ν)	30	10	10	10	1	1	1																																	
	ν_1	ν_2	ν_3	ν_4	ν_5	ν_6	ν_7																																																			
ac _{LB} ^{int} (ν)	0	0	0	0	0	0	0																																																			
ac _{UB} ^{int} (ν)	30	10	10	10	1	1	1																																																			
	<table border="1"> <thead> <tr> <th></th> <th>γ_1</th> <th>γ_2</th> <th>γ_3</th> <th>γ_4</th> <th>γ_5</th> <th>γ_6</th> <th>γ_7</th> <th>γ_8</th> <th>γ_9</th> <th>γ_{10}</th> <th>γ_{11}</th> <th>γ_{12}</th> <th>γ_{13}</th> <th>γ_{14}</th> <th>γ_{15}</th> <th>γ_{16}</th> <th>γ_{17}</th> <th>γ_{18}</th> </tr> </thead> <tbody> <tr> <td>ec_{LB}^{int}(γ)</td> <td>0</td> <td>0</td> <td>0</td> <td>0</td> <td>0</td> <td>0</td> <td>0</td> <td>0</td> <td>0</td> <td>0</td> <td>0</td> <td>0</td> <td>0</td> <td>0</td> <td>0</td> <td>0</td> <td>0</td> <td>0</td> </tr> <tr> <td>ec_{UB}^{int}(γ)</td> <td>4</td> <td>15</td> <td>4</td> <td>4</td> <td>10</td> <td>5</td> <td>4</td> <td>4</td> <td>6</td> <td>4</td> <td>4</td> <td>4</td> <td>2</td> <td>2</td> <td>2</td> <td>2</td> <td>2</td> <td>2</td> </tr> </tbody> </table>		γ_1	γ_2	γ_3	γ_4	γ_5	γ_6	γ_7	γ_8	γ_9	γ_{10}	γ_{11}	γ_{12}	γ_{13}	γ_{14}	γ_{15}	γ_{16}	γ_{17}	γ_{18}	ec _{LB} ^{int} (γ)	0	0	0	0	0	0	0	0	0	0	0	0	0	0	0	0	0	0	ec _{UB} ^{int} (γ)	4	15	4	4	10	5	4	4	6	4	4	4	2	2	2	2	2	2
	γ_1	γ_2	γ_3	γ_4	γ_5	γ_6	γ_7	γ_8	γ_9	γ_{10}	γ_{11}	γ_{12}	γ_{13}	γ_{14}	γ_{15}	γ_{16}	γ_{17}	γ_{18}																																								
ec _{LB} ^{int} (γ)	0	0	0	0	0	0	0	0	0	0	0	0	0	0	0	0	0	0																																								
ec _{UB} ^{int} (γ)	4	15	4	4	10	5	4	4	6	4	4	4	2	2	2	2	2	2																																								
	$\psi \in \{\psi_i \mid i = 1, 6, 11\} \quad \psi \in \mathcal{F}^* \setminus \{\psi_i \mid i = 1, 6, 11\}$																																																									
fc _{LB} (ψ)	1																																																									
fc _{UB} (ψ)	10																																																									
	$\nu \in \{(\text{C, C, 1}), (\text{C, C, 2})\} \quad \nu \in \Gamma_{\text{ac}}^{\text{lf}} \setminus \{(\text{C, C, 1}), (\text{C, C, 2})\}$																																																									
ac _{LB} ^{lf} (ν)	0																																																									
ac _{UB} ^{lf} (ν)	10																																																									

The lower bounds $\ell_{LB}, \text{bl}_{LB}, \text{ch}_{LB}, \text{bd}_{2, LB}, \text{bd}_{3, LB}, \text{na}_{LB}, \text{na}_{LB}^{\text{int}}, \text{ns}_{LB}^{\text{int}}, \text{ac}_{LB}^{\text{int}}, \text{ec}_{LB}^{\text{int}}$ and $\text{ac}_{LB}^{\text{lf}}$ are all set to be 0.

Set upper bounds $\text{na}_{UB}(\mathbf{a}) := n^*, \text{na} \in \{\text{H, C}\}, \text{na}_{UB}(\mathbf{a}) := 5, \text{na} \in \{\text{O, N}\}, \text{na}_{UB}(\mathbf{a}) := 2, \text{na} \in \Lambda \setminus \{\text{H, C, O, N}\}$. The other upper bounds $\ell_{UB}, \text{bl}_{UB}, \text{ch}_{UB}, \text{bd}_{2, UB}, \text{bd}_{3, UB}, \text{na}_{UB}^{\text{int}}, \text{ns}_{UB}^{\text{int}}, \text{ac}_{UB}^{\text{int}}, \text{ec}_{UB}^{\text{int}}$ and $\text{ac}_{UB}^{\text{lf}}$ are all set to be an upper bound n^* on $n(G^*)$.

We specify n_{LB} as a parameter and set $n^* := n_{LB} + 10, n_{LB}^{\text{int}} := \lfloor (1/4)n_{LB} \rfloor$ and $n_{LB}^{\text{int}} := \lfloor (3/4)n_{LB} \rfloor$.

For each property π , let $\mathcal{F}(\mathcal{C}_\pi)$ denote the set of 2-fringe-trees in the compounds in \mathcal{C}_π , and select a subset $\mathcal{F}_\pi^i \subseteq \mathcal{F}(\mathcal{C}_\pi)$ with $|\mathcal{F}_\pi^i| = 45 - 5i, i \in [1, 5]$. For each instance I_b^i , set

$$\mathcal{F}_E := \mathcal{F}(v) := \mathcal{F}_\pi^i, v \in V_C \text{ and } \text{fc}_{\text{LB}}(\psi) := 0, \text{fc}_{\text{UB}}(\psi) := 10, \psi \in \mathcal{F}_\pi^i.$$

Instance I_b^1 is given by the rank-1 seed graph G_C^1 in Figure 5(i) and Instances I_b^i , $i = 2, 3, 4$ are given by the rank-2 seed graph G_C^i , $i = 2, 3, 4$ in Figure 5(ii)-(iv).

- (i) For instance I_b^1 , select as a seed graph the monocyclic graph $G_C^1 = (V_C, E_C = E_{(\geq 2)} \cup E_{(\geq 1)})$ in Figure 5(i), where $V_C = \{u_1, u_2\}$, $E_{(\geq 2)} = \{a_1\}$ and $E_{(\geq 1)} = \{a_2\}$. We include a linear constraint $\ell(a_1) \leq \ell(a_2)$ and $5 \leq \ell(a_1) + \ell(a_2) \leq 15$ as part of the side constraint.
- (ii) For instance I_b^2 , select as a seed graph the graph $G_C^2 = (V_C, E_C = E_{(\geq 2)} \cup E_{(\geq 1)} \cup E_{(=1)})$ in Figure 5(ii), where $V_C = \{u_1, u_2, u_3, u_4\}$, $E_{(\geq 2)} = \{a_1, a_2\}$, $E_{(\geq 1)} = \{a_3\}$ and $E_{(=1)} = \{a_4, a_5\}$. We include a linear constraint $\ell(a_1) \leq \ell(a_2)$ and $\ell(a_1) + \ell(a_2) + \ell(a_3) \leq 15$.
- (iii) For instance I_b^3 , select as a seed graph the graph $G_C^3 = (V_C, E_C = E_{(\geq 2)} \cup E_{(\geq 1)} \cup E_{(=1)})$ in Figure 5(iii), where $V_C = \{u_1, u_2, u_3, u_4\}$, $E_{(\geq 2)} = \{a_1\}$, $E_{(\geq 1)} = \{a_2, a_3\}$ and $E_{(=1)} = \{a_4, a_5\}$. We include linear constraints $\ell(a_1) \leq \ell(a_2) + \ell(a_3)$, $\ell(a_2) \leq \ell(a_3)$ and $\ell(a_1) + \ell(a_2) + \ell(a_3) \leq 15$.
- (iv) For instance I_b^4 , select as a seed graph the graph $G_C^4 = (V_C, E_C = E_{(\geq 2)} \cup E_{(\geq 1)} \cup E_{(=1)})$ in Figure 5(iv), where $V_C = \{u_1, u_2, u_3, u_4\}$, $E_{(\geq 1)} = \{a_1, a_2, a_3\}$ and $E_{(=1)} = \{a_4, a_5\}$. We include linear constraints $\ell(a_2) \leq \ell(a_1) + 1$, $\ell(a_2) \leq \ell(a_3) + 1$, $\ell(a_1) \leq \ell(a_3)$ and $\ell(a_1) + \ell(a_2) + \ell(a_3) \leq 15$.

We define instances in (c) and (d) in order to find chemical graphs that have an intermediate structure of given two chemical cyclic graphs $G_A = (H_A = (V_A, E_A), \alpha_A, \beta_A)$ and $G_B = (H_B = (V_B, E_B), \alpha_B, \beta_B)$. Let Λ_A^{int} and $\Lambda_{\text{dg},A}^{\text{int}}$ denote the sets of chemical elements and chemical symbols of the interior-vertices in G_A , Γ_A^{int} denote the sets of edge-configurations of the interior-edges in G_A , and \mathcal{F}_A denote the set of 2-fringe-trees in G_A . Analogously define sets Λ_B^{int} , $\Lambda_{\text{dg},B}^{\text{int}}$, Γ_B^{int} and \mathcal{F}_B in G_B .

- (c) $I_c = (G_C, \sigma_{\text{int}}, \sigma_{\text{ce}})$: An instance aimed to infer a chemical graph G^\dagger such that the core of G^\dagger is equal to the core of G_A and the frequency of each edge-configuration in the non-core of G^\dagger is equal to that of G_B . We use chemical compounds CID 24822711 and CID 59170444 in Figure 6(a) and (b) for G_A and G_B , respectively.

Set a seed graph $G_C = (V_C, E_C = E_{(=1)})$ to be the core of G_A .

Set $\Lambda := \{\text{H}, \text{C}, \text{N}, \text{O}\}$, and set $\Lambda_{\text{dg}}^{\text{int}}$ to be the set of all possible chemical symbols in $\Lambda \times [1, 4]$.

Set $\Gamma^{\text{int}} := \Gamma_A^{\text{int}} \cup \Gamma_B^{\text{int}}$ and $\Lambda^*(v) := \{\alpha_A(v)\}$, $v \in V_C$.

Set $n_{\text{LB}}^{\text{int}} := \min\{n^{\text{int}}(G_A), n^{\text{int}}(G_B)\}$, $n_{\text{UB}}^{\text{int}} := \max\{n^{\text{int}}(G_A), n^{\text{int}}(G_B)\}$,

$n_{\text{LB}} := \min\{n(G_A), n(G_B)\} - 10 = 40$ and $n^* := \max\{n(G_A), n(G_B)\} + 5$.

Set lower bounds ℓ_{LB} , bl_{LB} , ch_{LB} , $\text{bd}_{2,\text{LB}}$, $\text{bd}_{3,\text{LB}}$, na_{LB} , $\text{na}_{\text{LB}}^{\text{int}}$, $\text{ns}_{\text{LB}}^{\text{int}}$, $\text{ac}_{\text{LB}}^{\text{int}}$ and $\text{ac}_{\text{LB}}^{\text{lf}}$ to be 0.

Set upper bounds $\text{na}_{\text{UB}}(\mathbf{a}) := n^*$, $\text{na} \in \{\text{H}, \text{C}\}$, $\text{na}_{\text{UB}}(\mathbf{a}) := 5$, $\text{na} \in \{\text{O}, \text{N}\}$, $\text{na}_{\text{UB}}(\mathbf{a}) := 2$, $\text{na} \in \Lambda \setminus \{\text{H}, \text{C}, \text{O}, \text{N}\}$ and set the other upper bounds ℓ_{UB} , bl_{UB} , ch_{UB} , $\text{bd}_{2,\text{UB}}$, $\text{bd}_{3,\text{UB}}$, $\text{na}_{\text{UB}}^{\text{int}}$, $\text{ns}_{\text{UB}}^{\text{int}}$, $\text{ac}_{\text{UB}}^{\text{int}}$ and $\text{ac}_{\text{UB}}^{\text{lf}}$ to be n^* .

Set $\text{ec}_{\text{LB}}^{\text{int}}(\gamma)$ to be the number of core-edges in G_A with $\gamma \in \Gamma^{\text{int}}$ and $\text{ec}_{\text{UB}}^{\text{int}}(\gamma)$ to be the number interior-edges in G_A and G_B with edge-configuration γ .

Let $\mathcal{F}_B^{(p)}$, $p \in [1, 2]$ denote the set of chemical rooted trees r-isomorphic p -fringe-trees in G_B ;

Set $\mathcal{F}_E := \mathcal{F}(v) := \mathcal{F}_B^{(1)} \cup \mathcal{F}_B^{(2)}$, $v \in V_C$ and $\text{fc}_{\text{LB}}(\psi) := 0$, $\text{fc}_{\text{UB}}(\psi) := 10$, $\psi \in \mathcal{F}_B^{(1)} \cup \mathcal{F}_B^{(2)}$.

(d) $I_d = (G_C^1, \sigma_{\text{int}}, \sigma_{\text{ce}})$: An instance aimed to infer a chemical monocyclic graph G^\dagger such that the frequency vector of edge-configurations in G^\dagger is a vector obtained by merging those of G_A and G_B . We use chemical monocyclic compounds CID 10076784 and CID 44340250 in Figure 6(c) and (d) for G_A and G_B , respectively. Set a seed graph to be the monocyclic seed graph $G_C^1 = (V_C, E_C = E_{(\geq 2)} \cup E_{(\geq 1)})$ with $V_C = \{u_1, u_2\}$, $E_{(\geq 2)} = \{a_1\}$ and $E_{(\geq 1)} = \{a_2\}$ in Figure 5(i).

Set $\Lambda := \{\text{H}, \text{C}, \text{N}, \text{O}\}$, $\Lambda_{\text{dg}}^{\text{int}} := \Lambda_{\text{dg},A}^{\text{int}} \cup \Lambda_{\text{dg},B}^{\text{int}}$ and $\Gamma^{\text{int}} := \Gamma_A^{\text{int}} \cup \Gamma_B^{\text{int}}$.

Set $n_{\text{LB}}^{\text{int}} := \min\{n^{\text{int}}(G_A), n^{\text{int}}(G_B)\}$, $n_{\text{UB}}^{\text{int}} := \max\{n^{\text{int}}(G_A), n^{\text{int}}(G_B)\}$,

$n_{\text{LB}} := \min\{n(G_A), n(G_B)\} = 40$ and $n^* := \max\{n(G_A), n(G_B)\}$.

Set lower bounds ℓ_{LB} , bl_{LB} , ch_{LB} , $\text{bd}_{2,\text{LB}}$, $\text{bd}_{3,\text{LB}}$, na_{LB} , $\text{na}_{\text{LB}}^{\text{int}}$, $\text{ns}_{\text{LB}}^{\text{int}}$, $\text{ac}_{\text{LB}}^{\text{int}}$ and $\text{ac}_{\text{LB}}^{\text{lf}}$ to be 0.

Set upper bounds $\text{na}_{\text{UB}}(\mathbf{a}) := n^*$, $\text{na} \in \{\text{H}, \text{C}\}$, $\text{na}_{\text{UB}}(\mathbf{a}) := 5$, $\text{na} \in \{\text{O}, \text{N}\}$, $\text{na}_{\text{UB}}(\mathbf{a}) := 2$, $\text{na} \in \Lambda \setminus \{\text{H}, \text{C}, \text{O}, \text{N}\}$ and set the other upper bounds ℓ_{UB} , bl_{UB} , ch_{UB} , $\text{bd}_{2,\text{UB}}$, $\text{bd}_{3,\text{UB}}$, $\text{na}_{\text{UB}}^{\text{int}}$, $\text{ns}_{\text{UB}}^{\text{int}}$, $\text{ac}_{\text{UB}}^{\text{int}}$ and $\text{ac}_{\text{UB}}^{\text{lf}}$ to be n^* .

For each edge-configuration $\gamma \in \Gamma^{\text{int}}$, let $x_A^*(\gamma^{\text{int}})$ (resp., $x_B^*(\gamma^{\text{int}})$) denote the number of interior-edges with γ in G_A (resp., G_B), $\gamma \in \Gamma^{\text{int}}$ and set

$x_{\text{min}}^*(\gamma) := \min\{x_A^*(\gamma), x_B^*(\gamma)\}$, $x_{\text{max}}^*(\gamma) := \max\{x_A^*(\gamma), x_B^*(\gamma)\}$,

$\text{ec}_{\text{LB}}^{\text{int}}(\gamma) := \lfloor (3/4)x_{\text{min}}^*(\gamma) + (1/4)x_{\text{max}}^*(\gamma) \rfloor$ and

$\text{ec}_{\text{UB}}^{\text{int}}(\gamma) := \lceil (1/4)x_{\text{min}}^*(\gamma) + (3/4)x_{\text{max}}^*(\gamma) \rceil$.

Set $\mathcal{F}_E := \mathcal{F}(v) := \mathcal{F}_A \cup \mathcal{F}_B$, $v \in V_C$ and $\text{fc}_{\text{LB}}(\psi) := 0$, $\text{fc}_{\text{UB}}(\psi) := 10$, $\psi \in \mathcal{F}_A \cup \mathcal{F}_B$.

We include a linear constraint $\ell(a_1) \leq \ell(a_2)$ and $5 \leq \ell(a_1) + \ell(a_2) \leq 15$ as part of the side constraint.